© 2015. Published by The Company of Biologists Ltd | Journal of Cell Science (2015) 128, 2231-2243 doi:10.1242/jcs.157867

RESEARCH ARTICLE

α-synuclein and synapsin III cooperatively regulate synaptic function in dopamine neurons

Michela Zaltieri[1], Jessica Grigoletto[1], Francesca Longhena[1], Laura Navarria[1], Gaia Favero[2], Stefania Castrezzati[2], Maria Alessandra Colivicchi[3], Laura Della Corte[3], Rita Rezzani[2], Marina Pizzi[1,7], Fabio Benfenati[4,5], Maria Grazia Spillantini[6], Cristina Missale[1], PierFranco Spano[1,7] and Arianna Bellucci[1,*]

ABSTRACT

The main neuropathological features of Parkinson's disease are dopaminergic nigrostriatal neuron degeneration, and intraneuronal and intraneuritic proteinaceous inclusions named Lewy bodies and Lewy neurites, respectively, which mainly contain α-synuclein (α-syn, also known as SNCA). The neuronal phosphoprotein synapsin III (also known as SYN3), is a pivotal regulator of dopamine neuron synaptic function. Here, we show that α-syn interacts with and modulates synapsin III. The absence of α-syn causes a selective increase and redistribution of synapsin III, and changes the organization of synaptic vesicle pools in dopamine neurons. In α-syn-null mice, the alterations of synapsin III induce an increased locomotor response to the stimulation of synapsin-dependent dopamine overflow, despite this, these mice show decreased basal and depolarization-dependent striatal dopamine release. Of note, synapsin III seems to be involved in α-syn aggregation, which also coaxes its increase and redistribution. Furthermore, synapsin III accumulates in the caudate and putamen of individuals with Parkinson's disease. These findings support a reciprocal modulatory interaction of α-syn and synapsin III in the regulation of dopamine neuron synaptic function.

KEY WORDS: α-synuclein, Dopamine release, Parkinson's disease, Synapsin III, Synaptic vesicles

INTRODUCTION

α-synuclein (α-syn, also known as SNCA) deposition in Lewy bodies (LB), that with nigrostriatal dopamine neuron loss are the key neuropathological features of Parkinson's disease, is crucial for the normal synaptic function of these cells (Anichtchik et al., 2013; Bellucci et al., 2012). For instance, α-syn acts as a negative regulator of nigrostriatal dopaminergic neuron function (Abeliovich et al., 2000; Larsen et al., 2006). Studies on α-syn-null mice that carry a spontaneous deletion of the gene locus encoding α-syn (C57BL/6JOlaHsd mice; Specht and Schoepfer, 2001) and resemble α-syn-specific knockout mice in terms of dopamine release, dopamine transporter (DAT, also known as SLC6A3) expression, striatal dopamine reuptake (Chadchankar et al., 2011) and nigral dopamine neuron number (Garcia-Reitboeck et al., 2013) have shown that α-syn decreases the refilling rate of readily releasable dopamine pools (Yavich et al., 2004). The decrease of dopamine overflow in these mice is not dependent on dopamine D2 autoreceptors misfunctioning or changes in dopamine re-uptake (Chadchankar and Yavich, 2011), thus indicating that other molecules, affected by the absence of α-syn, contribute to this phenomenon. Similar to the absence of α-syn, the increase of its protein levels in the nigrostriatal system causes a decrease of vesicle density and reduces dopamine release, thus promoting motor deficits (Garcia-Reitbock et al., 2010; Gaugler et al., 2012; Lundblad et al., 2012; Tofaris et al., 2006).

Analogous to α-syn, a specific member of the synapsin phosphoprotein family (Cesca et al., 2010; Porton et al., 2011), synapsin III (also known as SYN3), negatively modulates dopamine release in nigrostriatal neurons (Kile et al., 2010) and can also control the size of the recycling vesicle pools in hippocampal neurons (Feng et al., 2002). Among the synapsins, synapsin III is believed to be the only isoform that regulates vesicular monoamine transporter 2 (VMAT-2)-positive vesicle pools in the striatum (Bogen et al., 2006). Moreover, previous studies have shown that the protein showing most sequence homology to synaptin III – synaptin I (of which there are two isoforms, synapsin Ia and synapsin Ib encoded by SYN1) – can interact with α-syn (Bellucci et al., 2011a; Maiya et al., 2007) and that the two proteins have similar distribution profiles in hippocampal neurons (Tao-Cheng, 2006). Therefore, we investigated whether synapsin III and α-syn interact, and whether the absence or aggregation of α-syn affects synapsin-III expression and distribution in dopaminergic neurons. Furthermore, we evaluated whether silencing of the gene encoding synapsin III modulated α-syn distribution.

We found that, in dopamine neurons, absence or aggregation of α-syn significantly affected the expression and subcellular distribution of synapsin III without altering those of synapsin I (hereafter referred to synapsin Ia/b because the antibody used did not distinguish the two isoforms). This was associated with a specific rearrangement of synaptic vesicle clusters, a significant reduction of basal and depolarization-dependent dopamine release, and with the onset of an increased locomotor response to the administration of cocaine – a substance known to mobilize synapsin-dependent dopamine-vesicle reserve pools (Venton et al., 2006). In agreement with the results in mice and in cultured neurons, here, we also identify a significant redistribution of synapsin III in the caudate and putamen of individuals with Parkinson's disease, as well as in the striatum of transgenic mice expressing human α-syn, which also show decreased dopamine release and redistribution of synaptic proteins (Bellucci et al., 2011a; Garcia-Reitbock et al., 2010). Finally, by silencing synapsin III *in vitro* we could prevent α-syn aggregation and the related

[1]Department of Molecular and Translational Medicine, University of Brescia, 25123, Brescia, Italy. [2]Department of Clinical and Experimental Sciences, University of Brescia, 25123, Brescia, Italy. [3]NEUROFARBA Department, University of Florence, 50139, Florence, Italy. [4]Department of Neuroscience and Brain Technologies, 16163, Italian Institute of Technology, Genoa, Italy. [5]Department of Experimental Medicine, University of Genoa, 16132, Genoa, Italy. [6]Department of Clinical Neuroscience, The Clifford Allbutt Building, University of Cambridge, Cambridge CB2 0QH, UK. [7]Neurorehabilitation Unit, IRCCS San Camillo Hospital (NHS-Italy), 30126, Venice Lido, Italy.

*Author for correspondence (arianna.bellucci@unibs.it)

Received 9 June 2014; Accepted 30 April 2015

Journal of Cell Science (2015) 128, 2231-2243 doi:10.1242/jcs.157867

redistribution of synaptic proteins. Our findings uncover, for the first time, an interaction between α-syn and synapsin III that regulates the arrangement of releasable vesicle pools and synaptic function in dopaminergic neurons.

RESULTS

Absence and aggregation of α-syn modifies the distribution of synapsin III and DAT without altering synapsin Ia/b

We first studied synapsin III and α-syn distribution in primary dopaminergic mesencephalic neurons, which were identified by immunolabeling DAT, from wild-type control and α-syn-null mice (Fig. 1A; supplementary material Fig. S2A). Neurons were cultured for 10 days in order to reach an optimal stage of polarization, differentiation and synaptic maturation, as shown by phase-contrast images and immunopositive staining for β-III tubulin (also known as TUBB3), MAP-2 and synaptophysin (supplementary material Fig. S1A–D). Although labeling of synapsin III, α-syn and DAT showed a punctate distribution in dendritic processes in neurons from control mice, primary dopaminergic neurons from α-syn-null mice showed a dense and uniform distribution of both DAT and synapsin III (Fig. 1A; supplementary material Fig. S2A). These differences were supported by a significant increase in the size of the synapsin-III- (Fig. 1B) and DAT-immunopositive areas (supplementary material Fig. S1F).

Glucose deprivation is known to induce α-syn aggregation and to modify the subcellular distribution of DAT in primary dopaminergic neurons (supplementary material Fig. S1E–G; Bellucci et al., 2008, 2011a). Indeed, urea-soluble α-syn aggregates (Bellucci et al., 2008) and thioflavin-S-positive α-syn inclusions (supplementary material Fig. S1E) can be found in glucose-deprived neurons. We thus investigated whether changes in the synapsin-III subcellular distribution also occurred in dopamine mesencephalic neurons after glucose deprivation. Glucose-deprived neurons from C57BL/6J control mice showed a more uniform pattern of α-syn, synapsin-III and DAT immunolabeling when compared with untreated cells, and similar to our observations in α-syn-null neurons, there was a loss of punctuate staining, as confirmed by densitometry analysis (Fig. 1B). In glucose-deprived neurons, uniform synapsin-III immunoreactivity also extended to cell bodies, where it partially colocalized with the staining of DAT (supplementary material Fig. S2A). Glucose deprivation did not affect the distribution of synapsin III or DAT in α-syn-null neurons, as confirmed by densitometry analysis (Fig. 1A,B; supplementary material Fig. S2B). We then investigated whether

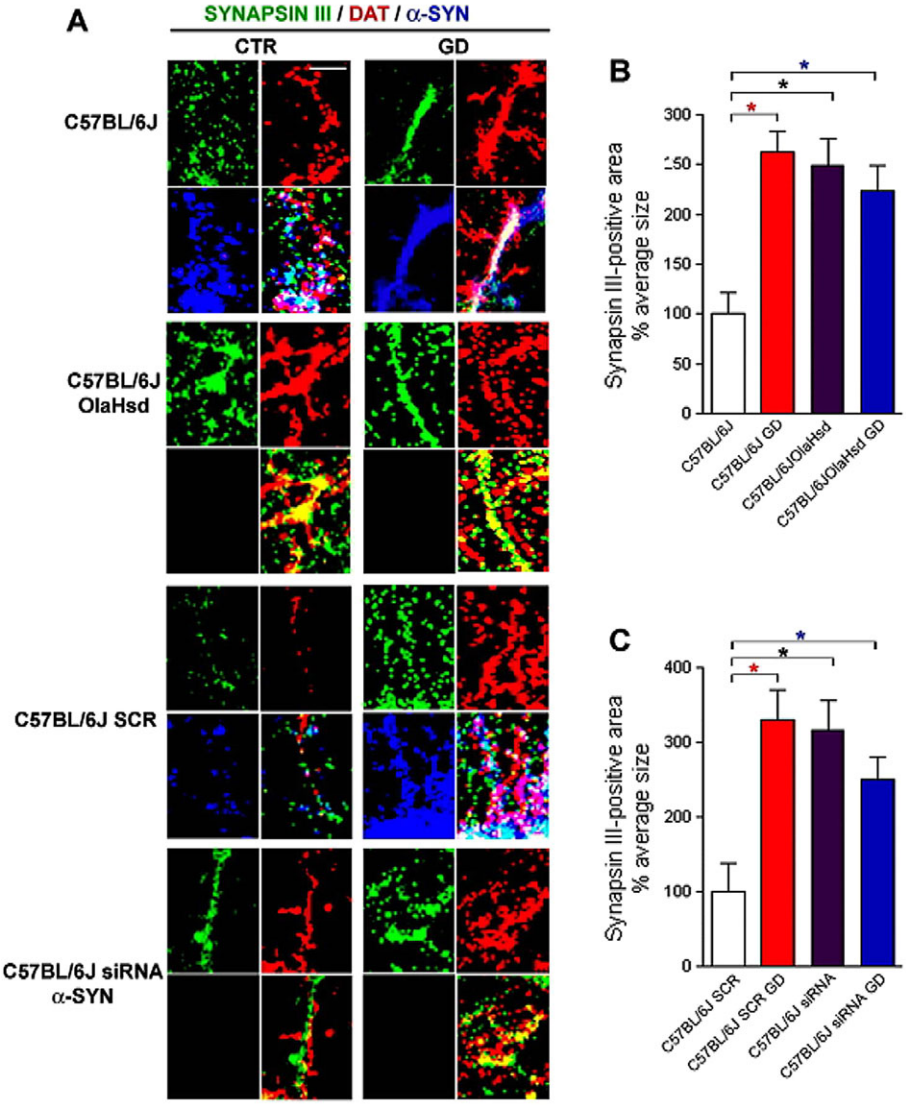

Fig. 1. Synapsin-III distribution in dopaminergic neurons. (A) Triple labeling of synapsin III, DAT and α-syn in primary mouse mesencephalic neurons in basal conditions and after glucose deprivation (GD). C57BL/6J and C57BL/6JOlaHsd neurons, as well as C57BL/6J neurons exposed to scrambled siRNA (SCR) or an siRNA against α-syn (siRNA α-syn), are presented. Scale bar: 10 µm. (B) Quantification of the percentage average size of the synapsin-III-immunopositive area in primary mouse mesencephalic dopaminergic neurons from C57BL/6J and C57BL/6JOlaHsd mice. **P*<0.001, **P*<0.05, **P*<0.05, one-way ANOVA with Tukey's multiple comparison test (mean±s.e.m., *n*=10 independent preparations for each condition repeated in triplicate). (C) Quantification of the percentage average size of the synapsin-III-immunopositive area in SCR- and α-syn-siRNA-transfected C57BL/6J primary mouse mesencephalic dopaminergic neurons. **P*<0.01, **P*<0.05, **P*<0.05. One-way ANOVA with Tukey's post test. (Mean±s.e.m., *n*=8 independent preparations for each condition repeated in triplicate).

Journal of Cell Science (2015) 128, 2231-2243 doi:10.1242/jcs.157867

synapsin Ia/b exhibited a similar localization to that of synapsin III. Synapsin Ia/b distribution was not influenced by the absence or aggregation of α-syn, as confirmed by image analysis (supplementary material Fig. S2A,B).

These findings indicate that the presence of α-syn selectively affects the distribution of synapsin III in primary mouse dopamine mesencephalic neurons. Moreover, the observation that glucose deprivation was able to significantly modulate the distribution of both DAT and synapsin III only in primary dopaminergic neurons from control mice suggests that α-syn has a direct modulatory effect on synapsin III.

To confirm that the alterations in synapsin-III and DAT distribution observed in neurons from α-syn null mice were due to the lack of α-syn and not to other compensatory mechanisms, we performed control experiments by inducing silencing of the gene encoding α-syn in neurons from control mice (Fig. 1A). Efficiency of the gene silencing was probed and confirmed by using real-time PCR (supplementary material Fig. S3I). Synapsin III showed a more intense and compact signal compared with that of untreated neurons when α-syn expression was silenced using small interfering (si) RNA. A similar result was obtained in scramble-siRNA (SCR)-transfected neurons when α-syn aggregation was induced by glucose deprivation. The distribution of synapsin III in neurons transfected with siRNA targeting the α-syn gene and deprived of glucose was not different from that of cells only transfected with siRNA against α-syn. These observations were confirmed by image-analysis studies (Fig. 1C). Similar changes were observed for DAT (supplementary material Fig. S3C). Of note, the distribution of synapsin Ia/b in cells exposed to siRNA against α-syn, glucose deprivation or the two together was not different compared with that of SCR-transfected control neurons (supplementary material Fig. S2A,C), thus reinforcing that α-syn does not directly modulate synapsin Ia/b distribution in dopaminergic neurons. Hence, the results obtained indicate that either the absence or the aggregation of α-syn selectively influences the subcellular distribution of synapsin III.

The distribution of synapsin III is altered in the striatum of SYN120-transgenic mice, and in the caudate and putamen of individuals affected by Parkinson's disease

We studied synapsin-III distribution in the striatum of 12-month-old control and α-syn-null mice, as well as that of transgenic mice expressing a C-terminally truncated form of human α-syn comprising only residues 1–120 of the protein (termed SYN120) on a mouse-α-syn-null background; we have previously used these mice to demonstrate that the absence or aggregation of α-syn can affect the distribution of synaptic vesicle proteins (Bellucci et al., 2011a; Garcia-Reitbock et al., 2010) (Fig. 2A). We found a marked increase of synapsin-III immunolabeling in the striatum of α-syn-null mice when compared with control mice. In addition, we observed that SYN120-transgenic mice showed a further concentration of synapsin-III immunolabeling in the striatum when compared with that of both control and α-syn-null mice. Double-immunofluorescence studies showed that synapsin III was not exclusively localized to the synaptic compartment as it only partially colocalized with synaptophysin (Fig. 2B).

Then, we performed staining of synapsin-III in the caudate and putamen of individuals affected by sporadic Parkinson's disease, and in age-matched control subjects. Specificity of the staining was confirmed by pre-adsorption of the antibody against synapsin III with human recombinant synapsin-III protein (supplementary material Fig. S4D), and by the different staining pattern of synapsin Ia/b in the caudate and putamen of control and disease-affected subjects (supplementary material Fig. S4E). Notably, we found a marked accumulation of synapsin-III staining in the brain of individuals with Parkinson's disease when compared with that of controls (Fig. 2C,D). Double-labeling immunofluorescence showed that in the caudate and putamen of individuals with Parkinson's disease, and of age-matched controls, synapsin III almost completely colocalized with α-syn (supplementary material Fig. S1H). In addition, we found that in the Parkinson-disease-affected striatum, as observed in the brain of SYN120-transgenic mice, synapsin III only partially colocalized with synaptophysin, differently from the control human brain, where the staining for the two proteins almost completely overlapped (supplementary material Fig. S1I). These findings indicate α-syn synaptic pathology in the caudate of individuals affected by Parkinson's disease that requires further investigation.

α-syn interacts with synapsin III, and the distribution of α-syn–synapsin-III complexes is affected by α-syn aggregation

Synapsin Ia/b is known to be a member of the α-syn interactome, but no study at present has investigated whether α-syn can bind to synapsin III. To test this interaction, we used the *in situ* proximity ligation assay (PLA) (Fig. 3A) (Bellucci et al., 2011a) and co-immunoprecipitation (Fig. 3B). Both methods showed a direct binding between α-syn and synapsin III in neurons from C57BL/6J control mice. Of note, the presence of a PLA-positive signal was not confined to DAT-positive cells, and we found an increased density of PLA red dots in both dopaminergic and non-dopaminergic control neurons that had been subjected to glucose deprivation, indicating a concurrent redistribution of α-syn–synapsin-III complexes in response to α-syn aggregation (Fig. 3A). After glucose deprivation, we observed a marked intensification of the PLA signal in the cell body, indicating the formation of intracellular aggregates comprising α-syn and synapsin III. The specificity of the PLA signal was confirmed by the absence of positive dots in neurons from α-syn-null mice and in control neurons when the assay was performed without adding either of the antibodies against synapsin III or α-syn (Fig. 3A).

Synapsin III levels are increased when α-syn is absent or aggregated

We then investigated whether the expression of synapsin III, synapsin Ia/b and DAT were altered in the absence of α-syn, or when α-syn aggregated following glucose deprivation (Fig. 4A–J). α-syn-null neurons showed a significant decrease of DAT (Fig. 4A,C) and a significant increase of synapsin-III levels (Fig. 4A,E) when compared with control neurons. A similar effect was observed after glucose deprivation (Fig. 4A,C,E). No difference was detected in the levels of synapsin Ia/b between α-syn-null and control neurons, both in basal conditions and after glucose deprivation (Fig. 4A,D). The experiments were repeated in neurons where α-syn expression had been silenced using siRNA, and following glucose deprivation. Similar to the results of previous experiments, a significant decrease of DAT levels (Fig. 4F,H) and an increase of synapsin III (Fig. 4F,J) were present with no effect on synapsin Ia/b levels (Fig. 4F,I). To exclude the possibility that the variations in the synapsin-III levels observed in primary neurons were due to non-dopaminergic neurons or glial cells present in the primary cell cultures, we evaluated the expression of synapsin III in a more uniform dopaminergic cell population – dopaminergic differentiated SH-SY5Y neuroblastoma cells (Bellucci et al., 2008) (supplementary material Fig. S3A–E). Similar to our observations in primary mesencephalic neurons, silencing of the α-syn gene and glucose deprivation decreased the levels of DAT (supplementary

Journal of Cell Science (2015) 128, 2231-2243 doi:10.1242/jcs.157867

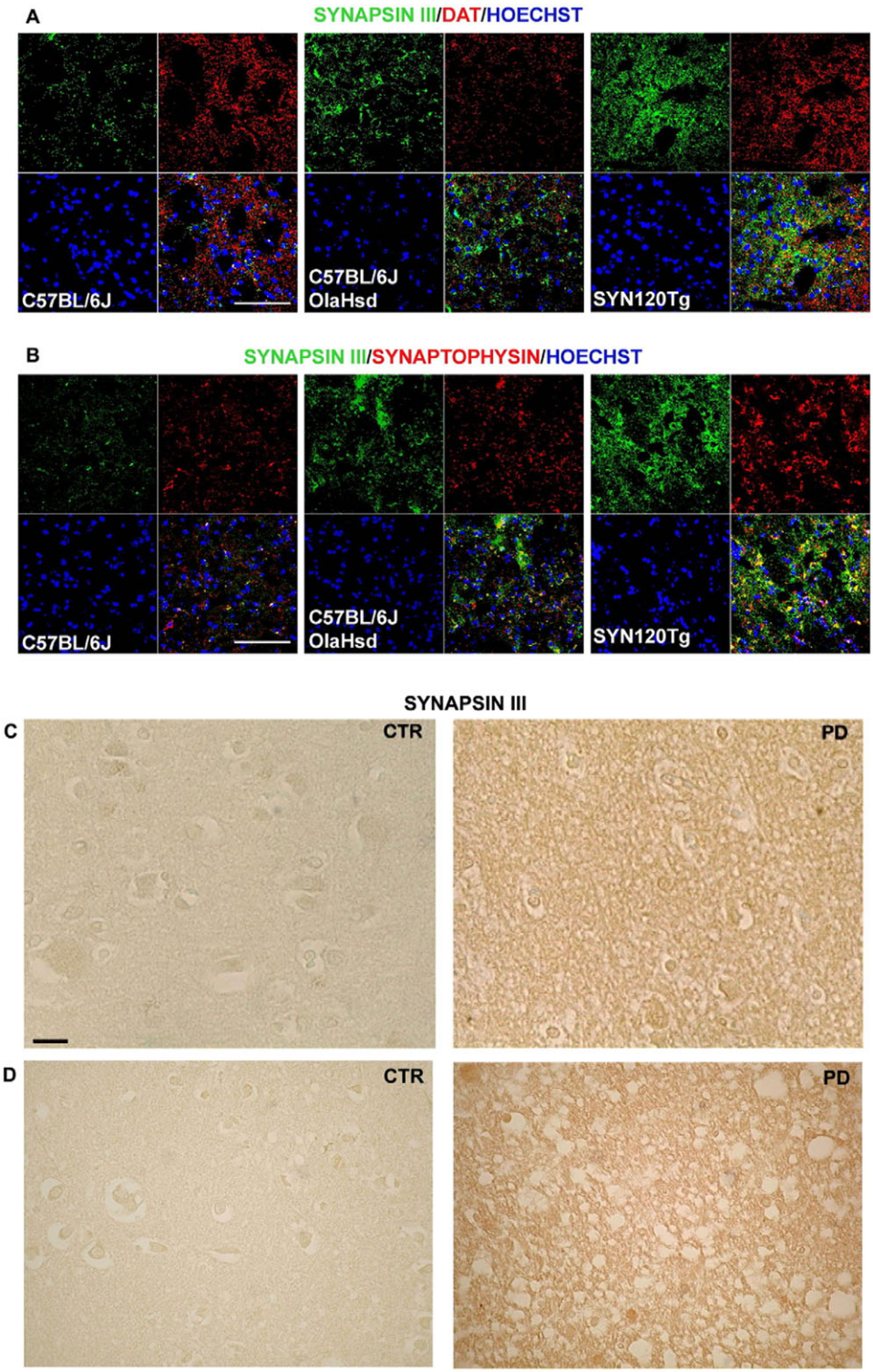

Fig. 2. Redistribution of synapsin III in the striatum of SYN120 mice, and in the caudate and putamen of individuals affected by sporadic Parkinson's disease. (A) Double-labeling of synapsin III and DAT in the striatum of C57BL/6J, C57BL/6JOlaHsd and SYN120 (SYN120Tg) mice. (B) Double-labeling of synapsin III and synaptophysin in the striatum of C57BL/6J, C57BL/6JOlaHsd and SYN120 mice. (C,D) Immunostaining of synapsin III in caudate and putamen brain slices of individuals affected by sporadic Parkinson's disease (PD) and age-matched controls (CTR). Images are representative of *n*=2 control brains and *n*=2 Parkinson's disease brains. Scale bars: 150 µm (A,B); 300 µm (C, also applicable to D).

material Fig. S3A,C) and increased the levels of synapsin III (supplementary material Fig. S3A,E), but did not affect synapsin Ia/b levels (supplementary material Fig. S3A,D).

Expression of C-terminally truncated α-syn modifies the subcellular distribution of both synapsin III and synapsin Ia/b

To confirm whether α-syn affected DAT and synapsin III distribution, besides their expression, we used a differentiated neuronal SK-N-SH cell line that stably expressed a green fluorescent protein (GFP)-conjugated form of DAT to overexpress the SYN120 mutant protein (Bellucci et al., 2011a). This form of α-syn can be found in LBs (Prasad et al., 2012), and promotes α-syn aggregation (Crowther et al., 1998), DAT redistribution (Bellucci et al., 2011a) and the induction of axonal and synaptic damage (Games et al., 2013; Garcia-Reitbock et al., 2010). We found that SYN120-expressing cells showed intracellular α-syn- and synapsin-III-immunopositive inclusions that contained DAT–GFP, whereas, in control SK-N-

Journal of Cell Science (2015) 128, 2231-2243 doi:10.1242/jcs.157867

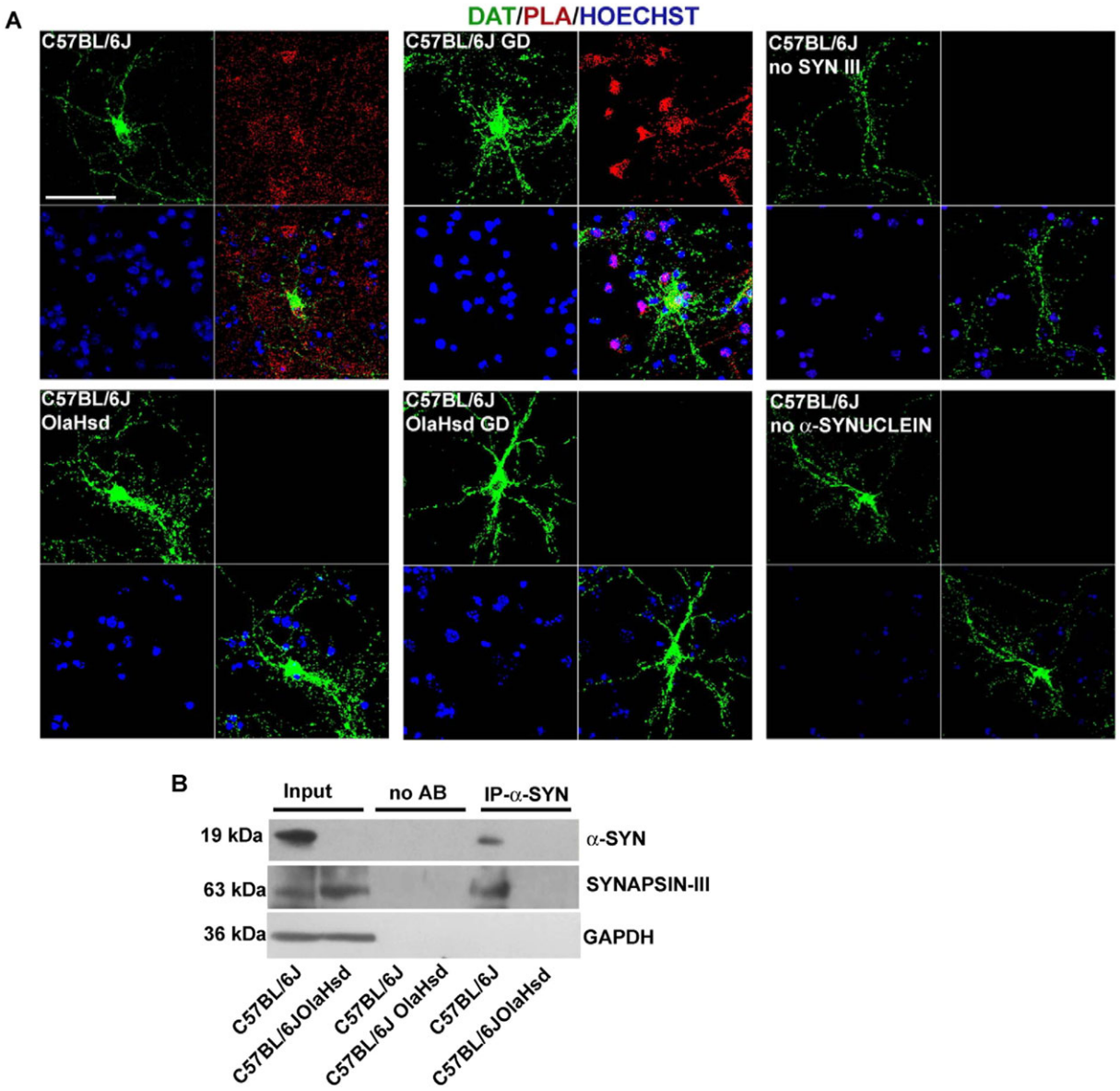

Fig. 3. Interaction of α-syn and synapsin III in dopaminergic neurons. (A) Representative images showing the PLA signal for synapsin-III–α-syn (PLA, red) and immunolabeling of DAT (green) in C57BL/6J and C57BL/6JOlaHsd mesencephalic neurons under basal conditions or after glucose deprivation (GD). Please note that the presence of a positive PLA signal is indicative of a synapsin-III–α-syn interaction in C57BL/6J neurons. The PLA signal was more concentrated when these neurons were deprived of glucose but was not detectable in C57BL/6JOlaHsd mice lacking α-syn under both basal conditions and glucose deprivation. Additionally, a PLA signal was not detected in C57BL/6J neurons when the PLA was performed without using either the antibody against synapsin III or α-syn ('no SYN III' and 'no α-SYNUCLEIN', respectively). Scale bar: 110 µm. (B) Representative western blot showing the presence of a synapsin-III-immunopositive band in α-syn-immunoprecipitated (IP-α-syn) protein samples from C57BL/6J mice. Input samples are representative of whole protein extracts from C57BL/6J and C57BL/6JOlaHsd mice. GAPDH bands are reported as a control for input samples. no AB, no antibody.

SH DAT–GFP cells, both synapsin III and DAT localized predominantly at the plasma membrane (supplementary material Fig. S3F). Intracellular inclusions that were triple-positive for α-synuclein, synapsin Ia/b and DAT–GFP were also found in SYN120-transfected cells, whereas, in control cells, synapsin Ia/b and DAT were mainly localized on the cell membrane (supplementary material Fig. S3G). These findings indicate that C-terminally truncated α-syn is able to modify the subcellular distribution of DAT, synapsin III and synapsin Ia/b. These characteristics were confirmed by using primary mesencephalic neuronal cell cultures prepared from SYN120-transgenic mice (M.Z. and A.B., unpublished observations).

An absence of α-syn alters vesicle clustering and induces synapsin-III accumulation in synaptic terminals

Next, we studied the arrangement of vesicle pools and the distribution of the different proteins in single synaptic terminals in our mesencephalic cell cultures by using ultrastructural morphological and immunogold transmission electron microscopy (TEM) analysis, respectively. A marked disorganization of synaptic vesicle pools was observed in proximity of the synaptic space in α-syn-null mesencephalic neurons and in control cells that had been subjected to α-syn gene silencing when compared with that in C57BL/6J control neurons (Fig. 5A). This was confirmed by a significant decrease in the number of synaptic vesicles per µm in the synaptic terminals of

Journal of Cell Science (2015) 128, 2231-2243 doi:10.1242/jcs.157867

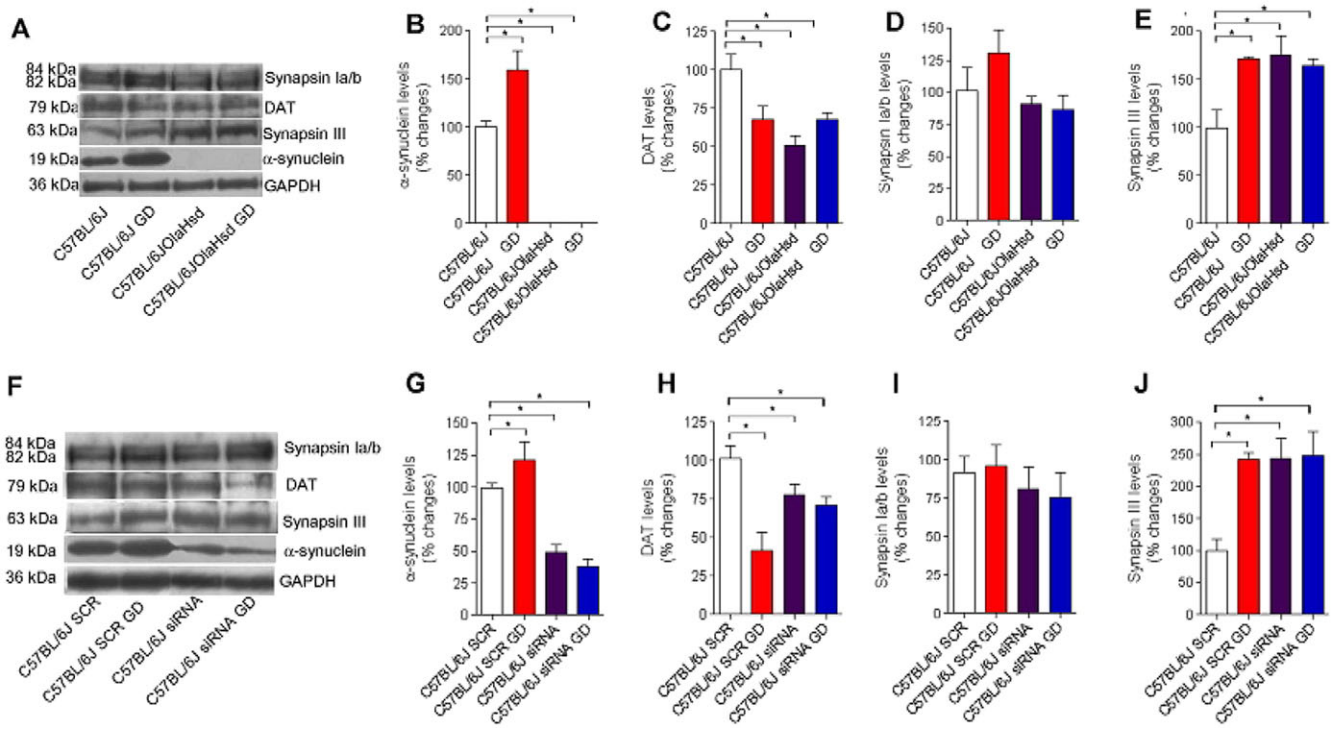

Fig. 4. Levels of α-syn, DAT, synapsin III and synapsin Ia/b in mesencephalic neurons. (A) C57BL/6J and C57BL/6JOlaHsd under basal conditions and after glucose deprivation ('GD'). (B–E) Levels of α-syn (B), DAT (C), synapsin Ia/b (D) and synapsin III (E) in C57BL/6J and C57BL/6JOlaHsd under basal conditions and after glucose deprivation. *P<0.05, one-way ANOVA with Tukey's post test (mean±s.e.m.; n=8 for each group). (F) C57BL/6J mesencephalic neurons exposed to a scrambled siRNA (SCR) or an siRNA against α-syn (siRNA) and then placed under basal conditions or glucose deprivation. (G–J) Levels of α-syn (G), DAT (H), synapsin Ia/b (I) and synapsin III (J) in SCR-siRNA- and α-syn-siRNA-exposed C57BL/6J mesencephalic neurons under basal conditions and after glucose deprivation. *P<0.05, one-way ANOVA with Tukey's post test (Mean±s.e.m.; n=8 for each group). GAPDH-immunopositive bands are a control for equal loading.

primary C57BL/6J neurons that had been subjected to glucose deprivation and of C57BL/6JOlaHsd neurons when compared with that of control C57BL/6J cells (Fig. 5C). By using immunogold labelling, we found that C57BL/6JOlaHsd mice and C57BL/6J mice that had been transfected with siRNA against α-syn showed larger areas of dense synapsin-III-positive staining in proximity to presynaptic membranes (Fig. 5B) when compared with that of C57BL/6J control neurons, which displayed weaker and more diffuse immunolabeling of synapsin III, as confirmed by the analysis of the distribution of synapsin-III-immunopositive grains (Fig. 5D). Interestingly, in C57BL/6JOlaHsd neurons, a significant reduction in the levels of DAT was present (supplementary material Fig. S4C), whereas no significant change was observed in immunogold labeling of synapsin Ia/b (supplementary material Fig. S4B).

α-syn-null mice display a reduction of basal and depolarization-dependent dopamine release but an increased locomotor response to cocaine administration

We proceeded to evaluate whether aged α-syn-null mice present differences in striatal synapsin-III and synapsin-Ia/b expression, as well as in basal and depolarization-induced dopamine release '*in vivo*'. Moreover we investigated the alterations in the locomotor response upon the administration of the selective DAT-blocker GBR-12935 or cocaine, which besides blocking DAT, also mobilizes the synapsin-dependent reserve pool of dopamine vesicles (Venton et al., 2006). We observed a statistically significant increase in the levels of synapsin III without changes in those if synapsin Ia/b in 12-month-old α-syn-null mice when compared with wild-type controls (Fig. 6A–C). By using vertical microdialysis in 12-month-old α-syn-null and wild-type mice, we found that, despite a significant reduction of DAT density and levels (Bellucci et al., 2011a) that could have been associated with increased striatal dopamine release, C57BL/6JOlaHsd mice showed a marked decrease of both basal and K^+-stimulated dopamine overflow when compared with control littermates (Fig. 6D). In addition, aged C57BL/6JOlaHsd mice displayed an increased locomotor response to the administration of cocaine (Fig. 6F), whereas, in agreement with their reduced levels of DAT, they showed a weaker response to the administration of GBR-12935 as compared with wild-type littermates (Fig. 6E). This evidence seems in line with previous findings that showed that repeated-burst stimulation, which redistributes vesicular storage pools and facilitates dopamine overflow, is enhanced in C57BL/6JOlaHsd mice (Chadchankar et al., 2012). The increased responsiveness of these mice to cocaine or repeated-burst stimulation might be explained by the selective increase of synapsin III in the striatum. Thus, despite the negative modulatory effect of synapsin III on basal and depolarization-dependent dopamine overflow, an increase in the level of this protein could enhance the responsiveness of reserve pools of vesicles to stimulation.

Silencing synapsin III prevents α-syn aggregation and the associated redistribution of synaptic proteins

To corroborate the reciprocal modulation of α-syn and synapsin III, we probed the effect of silencing of the gene encoding synapsin III on the subcellular distribution of α-syn in C57BL/6J mesencephalic neurons that had been deprived of glucose (Fig. 7). The efficiency of silencing synapsin III was probed and confirmed by using real-time

Journal of Cell Science (2015) 128, 2231-2243 doi:10.1242/jcs.157867

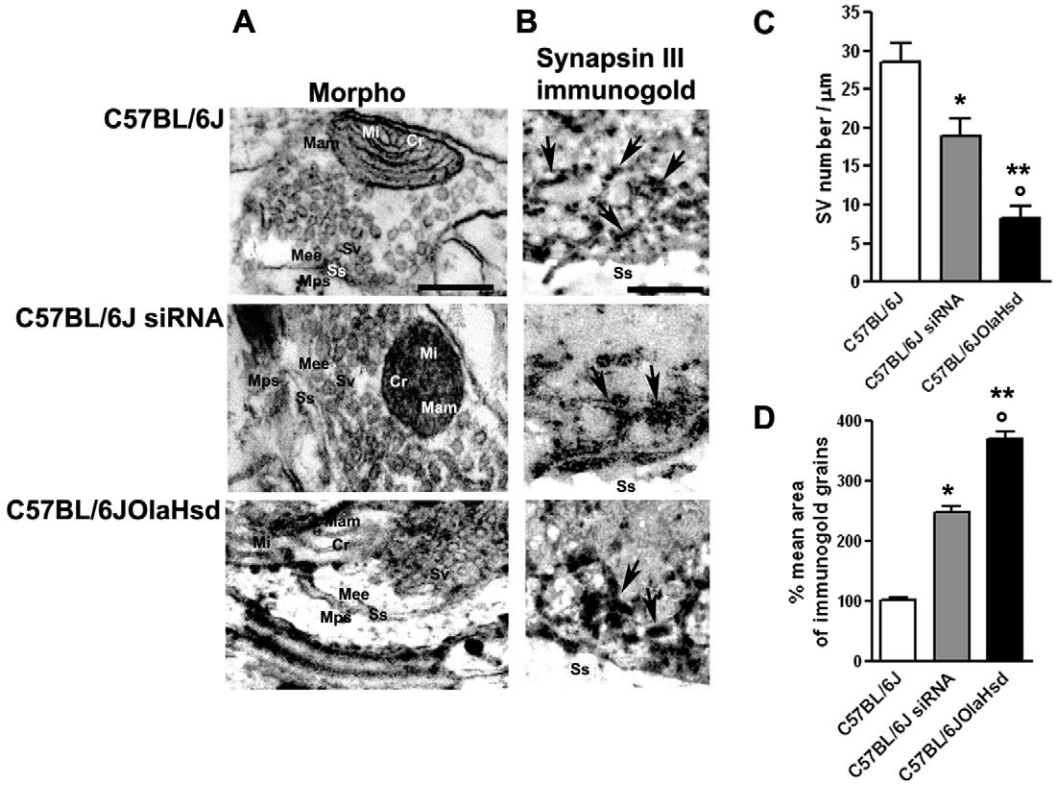

Fig. 5. A lack of α-syn perturbs synaptic vesicle clustering and synapsin-III distribution. (A) Different distribution of synaptic vesicles in C57BL/6J and C57BL/6JOlaHsd neurons under basal conditions, and in C57BL/6J neurons after silencing of the α-syn gene. Cr, mitochondrial cristae; Mam, mitochondrial matrix; Mee, pre-synaptic membrane; Mi, mitochondrion; Mps, post-synaptic membrane; Ss, synaptic space; Sv, synaptic vesicle. (B) Immunogold labeling of synapsin-III. Arrows indicate the immunogold-positive signal of synapsin III. (C) Synaptic vesicle distribution (expressed as number of synaptic vesicles/µm) in presynaptic boutons of C57BL/6J and C57BL/6JOlaHsd neurons, as well as in C57BL/6J mesencephalic neurons subjected to silencing of the α-syn gene (siRNA). **P*<0.05, ***P*<0.001 vs. C57BL/6J neurons, °*P*<0.05 vs. C57BL/6J siRNA, one-way ANOVA with Tukey's post test (mean±s.e.m.; *n*=15 different synapses from three different experiments were analyzed for each group). (D) Distribution of immunogold labeling of synapsin III (expressed as the percentage mean area of immunogold-positive grains) in presynaptic boutons of C57BL/6J and C57BL/6JOlaHsd neurons, as well as of C57BL/6J mesencephalic neurons subjected to silencing of the α-syn gene. **P*<0.001, ***P*<0.001 vs. C57BL/6J neurons, °*P*<0.05 vs. C57BL/6J siRNA, one-way ANOVA with Tukey's post test (mean±s.e.m.; *n*=10 or 15 different synaptic terminals from three different experiments were analyzed for each group). Scale bars: 500 nm (A); 50 nm (B).

PCR (supplementary material Fig. S3J). We found that silencing of the gene encoding synapsin III prevented the redistribution of α-syn that was induced by glucose deprivation (Fig. 7A), as confirmed by image analysis (Fig. 7B). In addition, in synapsin-III-silenced neurons that had been subjected to glucose deprivation, DAT distribution also appeared to be unchanged and showed a punctate appearance. Staining of synapsin Ia/b was unaffected by glucose deprivation alone or by glucose deprivation combined with silencing of synapsin III (supplementary material Fig. S3H). Of note, reducing the expression of synapsin III (Fig. 7D,E) prevented the increase in the levels of α-syn that was induced by glucose deprivation (Fig. 7D,G) without affecting those of synapsin Ia/b (Fig. 7D,F). In addition, silencing synapsin III impeded the formation of thioflavin-S- and α-syn-positive inclusions in glucose-deprived cells (Fig. 7C), suggesting that synapsin III plays a role in the induction of α-syn aggregation.

DISCUSSION

Collectively, these data show that α-syn and synapsin III cooperate in the regulation of dopamine neuron synaptic arrangement and neurotransmitter release. Our results indicate that either the absence or aggregation of α-syn induces an increase and redistribution of synapsin III in dopamine synapses that is associated with a failure of dopamine overflow (Fig. 8). Indeed, we found that the lack of α-syn in aged α-syn-null mice coincides with a decrease of both basal and depolarization-dependent striatal dopamine release that occurs in parallel with a marked increase and redistribution of synapsin-III levels in this area. These findings are in line with previous studies that have indicated that synapsin III can negatively control striatal dopamine release (Kile et al., 2010). However, we also found that, despite their functional deficits, the α-syn-null animals showed an increased locomotor response to the administration of cocaine, which is able to mobilize a synapsin-dependent reserve pool of dopamine (Venton et al., 2006), suggesting that the increase of striatal synapsin III is responsible for this phenomenon. Indeed, the increased response to cocaine administration in these mice cannot be ascribed to inhibition of DAT as they had reduced striatal levels of DAT and did not respond to the administration of the specific DAT blocker GBR-12935. Given the fact that we found that synapsin-Ia/b levels in the striatum of α-syn-null mice were not changed with respect to controls, our studies of behavior suggest that cocaine could stimulate the locomotor activity of these animals by inducing the release of synapsin-III-regulated vesicle pools of dopamine. Interestingly, high doses of cocaine have been found to alter α-syn distribution (Brenz Verca et al., 2003) and to block the formation of intracellular α-syn inclusions (Bellucci et al., 2008). Cocaine abuse elevates α-syn levels in the human striatum (Qin et al., 2005), whereas overexpression of α-syn in the nucleus accumbens influences the behavior of rats in response to cocaine (Boyer and Dreyer, 2007). Furthermore, methylphenidate, which like cocaine is able to affect exocytotic

Journal of Cell Science (2015) 128, 2231-2243 doi:10.1242/jcs.157867

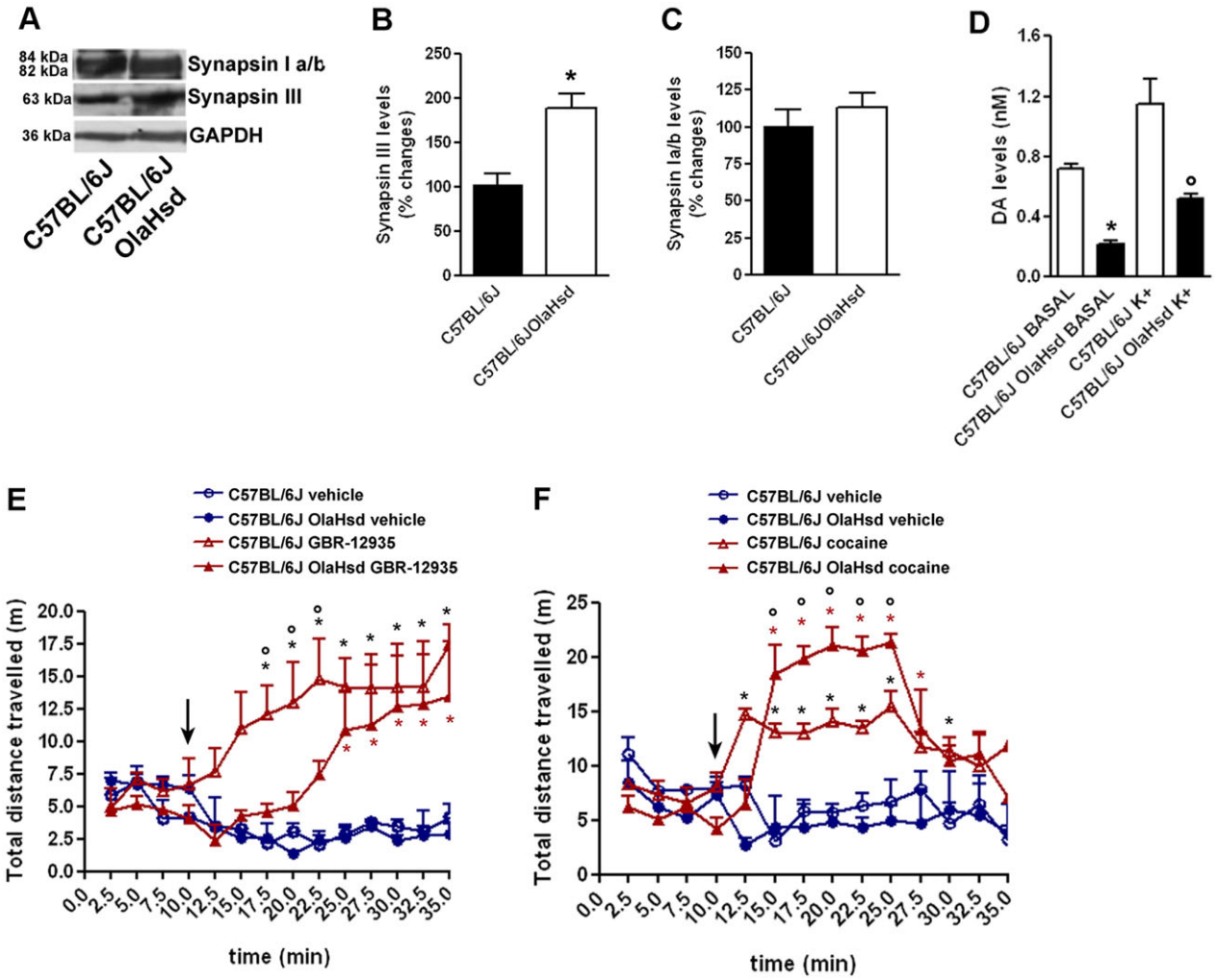

Fig. 6. α-syn-null mice show a marked increase of synapsin III in the striatum, decreased basal and depolarization-dependent dopamine release, and a super-locomotor response to cocaine administration. (A) Representative immunoblotting showing synapsin-III and synapsin-Ia/b levels in the striatum of 12-month-old C57BL/6J and C57BL/6JOlaHsd mice. GAPDH-immunopositive bands are a control for equal loading. (B) Histogram showing the quantification of the density of synapsin-III-immunopositive bands in 12-month-old C57BL/6J and C57BL/6JOlaHsd mice. Note the statistically significant increase in synapsin-III levels in α-syn-null mice, **P*<0.05, Student's *t*-test (mean±s.e.m.; *n*=8 for each group). (C) Histogram showing the quantification of the density of synapsin-Ia/b-immunopositive bands in 12-month-old C57BL/6J and C57BL/6JOlaHsd mice (mean±s.e.m.; *n*=8 for each group). No significant difference was observed. (D) Basal and K^+-stimulated dopamine ('DA') release in 12-month-old C57BL/6J and C57BL/6JOlaHsd mice. **P*<0.05 vs. C57BL/6J, °*P*<0.05 vs. C57BL/6J K^+, one-way ANOVA with Bonferroni's post test. (Mean±s.e.m.; *n*=8 for each group.) (E,F) Effect of GBR-12935 or cocaine administration on the locomotor activity of 12-month-old C57BL/6J and C57BL/6JOlaHsd mice evaluated as the total distance traveled in 35 min in the open field test. (E) Effect of the intraperitoneal administration of 10 mg/kg of GBR-12935 on the locomotor activity of 12-month-old C57BL/6J and C57BL/6JOlaHsd mice (group: $F_{3,94}$=30.82, *P*<0.0001; time: $F_{13,94}$=12.98, *P*<0.0001; interaction: $F_{39,94}$=39.90, *P*<0.0001; **P*<0.01 C57BL6J GBR12935 vs. C57BL/6J vehicle; **P*<0.05 C57BL6JOlaHsd GBR12935 vs. C57BL/6JOlaHsd vehicle; °*P*<0.05 C57BL6J GBR12935 vs. C57BL/6JOlaHsd GBR-12935, two-way ANOVA with Bonferroni's post comparison test, *n*=8 for each group). The arrow indicates GBR-12935 administration. (F) Effect of the intraperitoneal administration of 10 mg/kg of cocaine on the locomotor activity of 12-month-old C57BL/6J and C57BL/6JOlaHsd mice (group: $F_{3,84}$=41.28, *P*<0.0001; time: $F_{13,84}$=9.97, *P*<0.01; interaction: $F_{39,84}$=29.39, *P*<0.0001; **P*<0.05 C57BL6J cocaine vs. C57BL/6J vehicle; **P*<0.05 C57BL6JOlaHsd cocaine vs. C57BL/6JOlaHsd vehicle; °*P*<0.05 C57BL6J cocaine vs. C57BL/6JOlaHsd cocaine. Two-way ANOVA with Bonferroni's post comparison test, *n*=8 for each group). The arrow indicates cocaine administration.

dopamine release from synaptic vesicles (Volz et al., 2008), modifies overflow and presynaptic compartmentalization of dopamine through an α-syn-dependent mechanism (Chadchankar et al., 2012). All of these results suggest that drugs which mobilize dopamine vesicle pools act by regulating the function of α-syn–synapsin-III complexes. Therefore, in dopaminergic neurons, the cooperative action of α-syn and synapsin III could tune dopamine release, and the specific modulatory function of α-syn on synapsin III could govern synaptic vesicle arrangement. These data do not exclude the possibility that, in other neuronal populations where synaptic vesicle release is more selectively dependent on the function of other synapsins, α-syn cooperates with the other isoforms in a different manner.

A recent study has shown that the overexpression of α-syn induces a decrease of synaptic vesicle exocytosis that is greater in primary rat midbrain neurons than in hippocampal neurons (Nemani et al., 2010). Although the mechanisms underlying these differences still remain to be elucidated, it must be mentioned that synapsins differentially control synaptic vesicle release in different neuronal cell populations and that they also display specific localization sites within neurons (Cesca et al., 2010; Kile et al., 2010). Indeed, synapsin-I- and synapsin-II-knockout mice display marked changes in glutamate and γ-aminobutyric acid (GABA) neurotransmission but no evident alteration in VMAT-2-positive striatal synaptic vesicles (Bogen et al., 2006); a marked

Journal of Cell Science (2015) 128, 2231-2243 doi:10.1242/jcs.157867

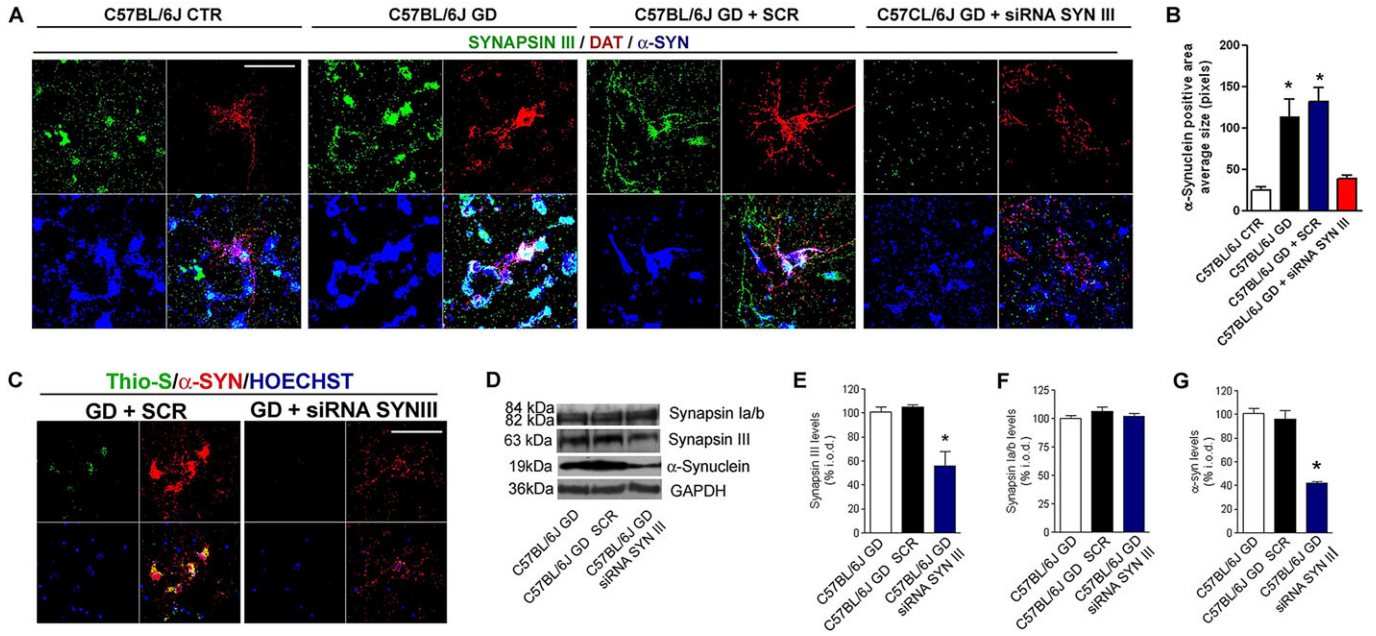

Fig. 7. Synapsin III modulates α-syn aggregation and distribution without affecting synapsin Ia/b. (A) Triple immunofluorescent labeling of synapsin III, DAT and α-syn in primary control C57BL/6J mesencephalic neurons or those exposed to glucose deprivation (GD), glucose deprivation and a scrambled siRNA (SCR), or glucose deprivation and an siRNA against synapsin III (siRNA SYN III). (B) Quantification of the percentage average size of the α-syn-immunopositive area under the various experimental conditions analyzed. **P*<0.05, one-way ANOVA with Tukey's multiple comparison test (mean±s.e.m.; *n*=6 independent preparations for each condition repeated in triplicate). (C) Thioflavin-S and α-syn double-labeling in C57BL/6J neurons that had been deprived of glucose and transfected with the SCR siRNA or that had been deprived of glucose and transfected with the siRNA against synapsin III. (D) Representative immunoblotting for synapsin Ia/b, synapsin III, α-syn and GAPDH in C57BL/6J mesencephalic neurons subjected to the indicated conditions. (E–G). Histograms showing the quantification of the density of synapsin-III- (E), synapsin-Ia/b- (F) and α-syn-immunopositive (G) bands in C57BL/6J mesencephalic neurons subjected to the indicated conditions. **P*<0.05, one-way ANOVA with Tukey's multiple comparison test. Scale bars: 100 µm (A); 120 µm (C). CTR, control.

increase of striatal dopamine release has been described in synapsin-III-knockout mice (Kile et al., 2010). Furthermore, in the adult brain, synapsin I and synapsin II are mainly found to be confined to synapses, but synapsin-III localization is extended to extrasynaptic sites, such as the soma and growth cones (Porton et al., 2011), suggesting that this isoform is not exclusively implicated in synaptic transmission. Along this line, our findings indicate that synapsin III is implicated in α-syn aggregation, although the molecular features of this effect warrant further investigation. To date, α-syn overexpression in transgenic mice has been found to associate with a decrease in synapsin-Ia/b, synapsin-IIa/b and complexin-2 levels in whole brain extracts (Nemani et al., 2010), and its aggregation at cortical synapses induces a decrease of synapsin-I levels (Spinelli et al., 2014), but no study has determined whether α-syn is able to modulate synapsin III at present. Here, we have shown that α-syn interacts with and specifically modulates synapsin III in primary midbrain neurons. Indeed, mesencephalic cells that lack α-syn show alterations in synaptic vesicle clustering in parallel with a marked concentration of synapsin III at synaptic boutons; however, these changes are not associated with alterations in synapsin Ia/b arrangement and expression. We also found that the expression of SYN120 in SK-N-SH-DAT-GFP cells modifies the distribution of synapsin Ia/b, suggesting that post-translational modifications of α-syn, such as C-terminal truncation, might also promote aggregation and enlarge its window of action at the synapse, with still more devastating consequences for the maintenance of proper synaptic homeostasis. The deletion of the C-terminus of α-syn does not affect the ability of the protein to inhibit synaptic vesicle exocytosis (Nemani et al., 2010), but it might still induce other alterations of synaptic physiology. For instance, C-terminally truncated α-syn is not able to bind to synaptobrevin II and to promote assembly of SNARE complexes (Burre et al., 2010).

Of note, selective changes in synapsin III were observed in neurons where α-syn aggregation had been induced by glucose deprivation. We have previously shown that glucose deprivation, which mimics decreasing energy supply in the ageing brain, induces the formation of α-syn insoluble aggregates, decreases dopamine cell viability and alters their function (Bellucci et al., 2008, 2011a). In addition, we have shown that glucose deprivation is also able to induce α-syn aggregation within the endoplasmic reticulum (ER). The binding of α-syn aggregates to the ER-stress sensor glucose regulated protein 78 (GRP78) then induces the unfolded protein response (UPR) (Bellucci et al., 2011b), an ER-stress response that is activated in Parkinson's-disease-affected brains. Prolonged activation of the UPR blocks ER–Golgi trafficking. This phenomenon might impair the generation and repackaging of synaptic vesicles, as well as the trans Golgi network (TGN)-mediated proper trafficking of proteins to the synaptic compartment (Bellucci et al., 2012). In addition, GRP78 clustering at the cell surface of neurons can mediate the α-syn-induced dysregulation of actin turnover, which can lead to early deficits in synaptic functions that precede neurodegeneration (Bellani et al., 2014). We cannot at present exclude that, at least in part, the observed redistribution and accumulation of synaptic proteins in our experimental models, and in the Parkinson's disease brain might be related to the activation of the UPR or to alterations of actin turnover.

In relation to α-syn aggregation, our observations indicate that this event affects synapsin-III distribution and expression. Moreover, we found that neurons that had been exposed to glucose deprivation showed a marked increase in the PLA-positive signal both in the processes and cell soma, which might

Journal of Cell Science (2015) 128, 2231-2243 doi:10.1242/jcs.157867

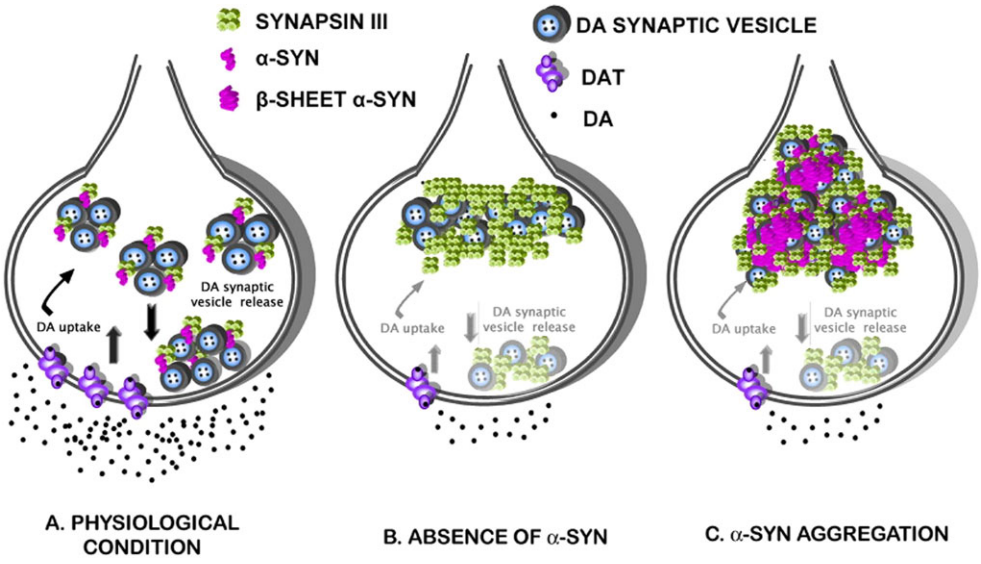

Fig. 8. The dopaminergic terminal with and without α-syn. (A) Putative organization of a presynaptic dopamine (DA) terminal under physiological conditions. (B) The absence of α-syn decreases the amount of membrane DAT and increases the density of synapsin III in presynaptic boutons, thus altering the proper clustering of synaptic vesicles at the active zone. This coincides with a reduction of dopamine release. (C) Aggregation of α-syn might determine a rearrangement of dopamine terminals, similar to its absence. A marked reduction of DAT, a significant accumulation of synapsin III and a collapse of synaptic vesicle pools coinciding with the reduction of their clustering at the active zone could reduce dopamine release.

indicate the formation of large α-syn- and synapsin-III-positive aggregates within these cells. It is thus likely that the sequestration of α-syn and synapsin III into intracellular aggregates determines the loss of their functions, thus altering synaptic vesicle arrangement and inducing a reduction of dopamine release (Fig. 8). In line with this hypothesis, the acute increase in the levels of α-syn has been found to inhibit the synaptic vesicle recycling that is evoked during intense stimulation (Busch et al., 2014), and cells that overexpress α-syn show a smaller population of readily releasable vesicles that correlates with reduced depression of evoked release in response to repeated stimuli (Larsen et al., 2006). Remarkably, we also showed a marked redistribution of synapsin III in the striatum of SYN120-transgenic mice and found that the protein accumulated and almost completely colocalized with α-syn in the caudate and putamen of individuals with Parkinson's disease. In addition, we observed that in this area synapsin III did not exclusively colocalize with the synaptic marker synaptophysin. This finding either indicates the occurrence of a spreading of α-syn pathology beside its redistribution or confirms the development of α-syn-immunoreactive astrocytes, which have been previously described by Braak and colleagues (Braak et al., 2007). Finally, we found that silencing of synapsin III prevents α-syn aggregation and blocks the related redistribution of synaptic proteins, thus suggesting a role for synapsin III in the process. This evidence, coupled to the observations of the Parkinson's disease brain, strongly supports the idea that synapsin III is involved in α-syn aggregation.

Altogether, our observations indicate that synapsin III can function as an accessory protein for the α-syn-related regulation of dopamine synaptic vesicle arrangement and suggest that the loss of function of α-syn, deriving from its aggregation, might further contribute to the dysfunction of dopamine synapses in light of the lack of α-syn–synapsin-III-mediated control of synaptic vesicles. These findings have important implications in the field of Parkinson's disease pathophysiology and therapeutic intervention.

MATERIALS AND METHODS

Animals

C57BL/6JOlaHsd mice (α-syn null) at 12 months of age (Harlan Olac, Bicester, UK) carrying a spontaneous deletion of the α-syn locus (Specht and Schoepfer, 2001), mice transgenic for SYN120 (Garcia-Reitbock et al., 2010; Tofaris et al., 2006) and wild-type C57BL/6J control mice (Charles River, Wilmington, MA) were used for this study. The mice were bred and housed in the animal-house facility of the Department of Molecular and Translational Medicine of the University of Brescia. The animals had *ad libitum* food and water, and were maintained under a 12-h light–dark cycle at a room temperature of 23°C. All experiments were performed according to Directive 2010/63/EU of the European Parliament and of the Council of 22 September 2010 on the protection of animals used for scientific purposes. All experimental and surgical procedures conformed to the National Research Guide for the Care and Use of Laboratory Animals and were approved by the Animal Research Committees of the University of Brescia (Protocol Permit number 03/12 and 04/12). All efforts were made to minimize animal suffering and to reduce the number of animals used.

Cell cultures

Primary embryonic mouse ventral mesencephalic cells were isolated and cultured as previously described (Bellucci et al., 2008) with minor modifications. Briefly, ventral mesencephalic tissues were dissected from C57BL/6J and C57BL/6JOlaHsd mice at embryonic day 13.5. After mechanical dissociation, the single cell suspension was resuspended in Neurobasal medium (Gibco, Milan, Italy) containing 100 µg/ml penicillin, 100 µg/ml streptomycin (Sigma-Aldrich, Milan, Italy), 2 mM glutamine (EuroClone, Milan, Italy) and 1% B27 supplement (Gibco); cells were then centrifuged. Cell count and viability assays were performed using the Trypan Blue exclusion test. Cells were seeded onto poly-D-lysine-coated glass coverslides in 24-well plates for immunocytochemistry, or onto poly-D-lysine coated Petri dishes for western blot or transmission electron microscopy analyses. Cells were maintained at 37°C under a humidified atmosphere of 5% CO_2 and 95% O_2 in Neurobasal medium for 10 days *in vitro*.

Human neuroblastoma SH-SY5Y cells (American Type Culture Collection, Manassas, VA) were grown and differentiated as previously described (Bellucci et al., 2008). For immunocytochemistry and western blot analysis, cells were seeded either onto poly-D-lysine-coated Petri dishes or onto poly-D-lysine-coated glass coverslides in 24-well plates, respectively.

Human neuroblastoma SK-N-SH cells were grown to confluence in complete medium comprising Dulbecco's modified Eagle's medium with 1000 mg glucose/l supplemented with 10% heat-inactivated fetal bovine serum, 100 µg/ml penicillin, 100 µg/ml streptomycin and 0.01 µM non-essential amino acids. Cells were maintained at 37°C under a humidified atmosphere of 5% CO_2 and 95% O_2. Neuron-like differentiation was performed by incubating the cells for 10 days in 10 µM retinoic acid. For immunocytochemistry and western blot analysis, cells were seeded

(2×10^4 cells/cm^2) either onto poly-D-lysine-coated slides in 24-well plates or onto Petri dishes, respectively. Cells were grown to 60–80% confluence and then transfected to stably express a pcDNA 3.1 green fluorescent protein (GFP)-conjugated form of human DAT (a kind gift from Prof. Marc G. Caron, Howard Hughes Medical Institute, Durham, NC) using LyoVec™ (InvivoGen, San Diego, CA), according to the manufacturer's instructions. Positive clones were selected using Geneticin G418 (Sigma-Aldrich). Western blotting was used to assess the expression of the proteins of interest (data not shown).

Transfection of human SYN120 into SK-N-SH cells

SK-N-SH DAT-GFP stable clones were seeded onto poly-D-lysine-coated glass coverslides in 24-well plates and subsequently differentiated towards a dopaminergic phenotype, as previously described. Differentiated cells were then transiently transfected with a pcDNA 3.1 vector encoding human C-terminally truncated α-syn (comprising residues 1–120 of the protein, SYN120). Cells were grown to 60–80% confluence and transfected using LyoVec™ (InvivoGen). Immunostaining experiments were performed 72 h after transfection.

Triple-labeling immunocytochemistry

For immunostaining experiments, cells were fixed by incubating for 10 min in 4% paraformaldehyde with 4% sucrose in 1 M PBS, pH 7.4; the fixed cells were then stored in PBS-containing 0.05% sodium azide. Slides were incubated for 4 h at room temperature in blocking solution [1% w/v bovine serum albumin (BSA) plus 10% v/v normal goat serum in PBS], then overnight at 4°C with the primary antibody at the optimal working dilution. On the following day, cells were incubated for 1 h at room temperature with the fluorochrome-conjugated secondary antibody diluted in 0.1% Triton X-100 PBS plus BSA 1 mg/ml. After three washes in 0.1% Triton X-100 PBS, cells were incubated for 2 h at room temperature with the second primary antibody, followed by incubation for 1 h at room temperature with the optimal secondary antibody. Cells were then washed three times and underwent another cycle of staining. Finally, cell nuclei were counterstained with Hoechst 33258 dye (Sigma-Aldrich), and the coverslips were mounted onto glass slides using Vectashield (Vector Laboratories, Burlingame, CA).

Immunohistochemistry

C57BL/6J, C57BL/6JOlaHsd and SYN120 mice were anesthetized with chloral hydrate (400 mg/kg intraperitoneally) (Sigma-Aldrich) and were perfused transcardially with 4% ice-cold paraformaldehyde in high molarity PBS [PBS A; normal saline 1.54 M + 2×PO_4 buffer (NaOH 0.2 M, NaH_2PO_4 0.2 M)]. After 4 h of post-fixation, brains were incubated in 18% sucrose for at least 24 h, and then 30-µm coronal sections were cut with a cryostat. Double-labeling immunohistochemistry was performed according to previously described methods (Bellucci et al., 2011a).

For staining of human sections, caudate and putamen from two controls (PDC008 and PDC022, average age 83 years, diagnosed with brainstem predominant α-synucleopathy) and two individuals with Parkinson's disease (PD016 and PD093, average age 73 years) were used (Parkinson's UK Brain Bank, Centre for Neuroscience, Imperial College London, London, UK). Following deparaffinization and antigen retrieval with buffer citrate 10 mM, the sections were incubated with primary antibody overnight at 4°C. Then, they were washed with PBS and incubated with biotinylated goat anti-rabbit IgG (Vector Laboratories, Burlingame, CA) for 45 min at room temperature. This was followed by four washes in PBS followed by incubation with avidin–biotin prepared in PBS with 0.1% Tween-20 (Vectastain ABC kit, Vector Laboratories) at room temperature. Following three washes in PBS, the reaction was visualized using 3,3′-diaminobenzidine. Sections were washed, dehydrated, mounted with Vestamount mounting medium (Vector Laboratories) and were observed by means of an inverted light/epifluorescence microscope (Olympus IX50; Olympus, Milan, Italy).

Antibodies

α-syn was visualized by using the following monoclonal antibodies: α-synuclein 211 (Santa Cruz Biotechnology, Santa Cruz, CA) and SYN-1 (BD-Biosciences, Milan, Italy), recognizing residues 121–125 of the human form, and residues 91–99 of the human and rat forms of α-syn, respectively. Anti-DAT (Santa Cruz Biotechnology), anti-synapsin Ia/b (Merck-Millipore®, Milan, Italy), anti-synaptophysin (Synaptic Systems, Goettingen, Germany) and anti-synapsin-III (Abcam, Cambridge, UK) polyclonal antibodies were used to visualize the respective substrates. An anti-glyceraldehyde-3-phosphate dehydrogenase (GAPDH) monoclonal antibody (Sigma-Aldrich) was used for western blot analyses. For immunoprecipitation studies, synapsin III was visualized by means of the RU486 synapsin-III-specific polyclonal antibody.

Confocal microscopy

Fixed cells were observed by means of an inverted light/epifluorescence microscope or of a Zeiss confocal laser microscope (Carl Zeiss S.p.A., Milan, Italy), with the laser set on λ=405–488–543 nm and the height of the sections scanning=1 µm. Images (512×512 pixels) were then reconstructed using LSM Image Examiner (Carl Zeiss S.p.A.) and Adobe Photoshop 7.0 (Adobe system, Mountain View, CA) software.

Analysis of protein density in DAT-positive neurons

Synapsin III, synapsin Ia/b and DAT density was performed by a blind rater that, for each slide, analyzed a minimum of ten fields (images were acquired at 63× magnification) containing DAT-positive neurons by using the ImageJ Software (NIH Image, USA). The threshold set-up was fixed between 30 and 150. The densitometry analysis is indicative of the percent average size of the α-syn, synapsin III, synapsin Ia/b and DAT-positive areas in the different fields analyzed. For image analysis, each experimental condition was performed in triplicate for each experiment, which was repeated at least eight times. The data were totaled and averaged for each of three replications. Data were expressed as a percentage with respect to the control untreated cells, plotted on graph and analyzed.

Glucose deprivation and RNA interference

Glucose deprivation was used to induce α-syn aggregation (Bellucci et al., 2008). siRNAs directed against human α-syn 5′-UGGCAACAGUG-GCUGAGAA-3′ (Dharmacon Thermo Scientific, Lafayette, CO) or synapsin III 5′-CAUGCAAGUUGUGAGAAA-3′ (Integrated DNA Technologies, Coralville, Iowa) were used to silence the target proteins. A non-targeting SCR siRNA was used as negative control for the different sequences. The optimal targeting and SCR RNA concentrations for α-syn gene silencing was estimated to be 25 nM, whereas that for synapsin III gene silencing was 5 nM. All the sequences were diluted in Opti-MEM (Gibco) and then transfected into cells using INTERFERin (Polyplus-transfection, Illkirch, France) according to the manufacturer's instructions. After 96 h of incubation in the case of α-syn and after 48 h for synapsin III, cells were fixed or scraped. The α-syn gene was silenced 2 days before glucose deprivation when the two parameters were used concomitantly. Synapsin III gene silencing was performed after glucose deprivation.

Western blotting and immunoprecipitation studies

For protein extraction, either SH-SY5Y cells or primary mesencephalic neuron pellets, as well as striatal brain tissue from C57BL/6J and C57BL/6JOlaHsd mice, were lysed in radioimmunoprecipitation (RIPA) buffer containing 50 mM Tris–HCl, pH 7.4, 150 mM NaCl, 1% NP-40 (Sigma-Aldrich), 0.5% sodium deoxycholate, 1 mM NaF, 1 mM Na_3VO_4 and 0.1% SDS, 1 mM PMSF, 2 mM EDTA plus complete proteasome inhibitor mixture (Roche Diagnostics, Mannheim, Germany), followed by centrifugation at 3000 ***g*** for 5 min at 4°C. Protein concentration in the samples was measured by using the Bio-Rad DC™ protein assay kit (Bio-Rad Laboratories, Milan, Italy). Equal amounts of protein (30 µg) were separated on 10% NuPAGE Novex Bis–Tris gels (Life-Technologies, Carlsbad, CA). Densitometry analysis of bands was performed by means of Gel Pro Analyzer version 6.0 (MediaCybernetics, Bethesda, MD). All bands were normalized to GAPDH levels as a control of equal loading of samples. For co-immunoprecipitation studies, equal amounts of total protein extracts (100 or 150 µg) were subjected to pre-clearing in ice-cold RIA buffer (400 mM NaCl, 20 mM EDTA, 20 mM Na_2HPO_4 and 1% NP-40), 0.1% SDS with 20 µl A/G Plus agarose beads (Santa Cruz Biotechnology) for 1 h under agitation at 4°C. Samples were then centrifuged for 5 min at 1000 ***g***,

Journal of Cell Science (2015) 128, 2231-2243 doi:10.1242/jcs.157867

and the resulting supernatant was then incubated for 2 h under agitation at 4°C with an anti-synapsin-III antibody. After adding 30 µl Protein A/G Plus agarose beads (Santa Cruz Biotechnology), samples were incubated with agitation over night at 4°C and then centrifuged at 1000 ***g*** for 2 min at 4°C. Pellets were washed four times with PBS, and then homogenized in 50 µl of sample buffer and run on a 10% NuPAGE Novex Bis-Tris gels (Invitrogen). For densitometry analysis of bands, each experimental condition was performed in triplicate at least eight times.

Proximity ligation assay

The *in situ* PLA studies on fixed cells were performed by using the Duolink assay kit (O-LINK Bioscience, Upsalla, Sweden) with a protocol adapted from the manufacturer's instruction for the co-labeling with DAT antibody. Briefly, fixed cells were incubated with blocking solution [3% w/v BSA plus 2% v/v normal goat serum in 0.1% Triton X-100 PBS) for 1 h and then with the primary antibodies recognizing synapsin III and α-syn at 1:200 dilution overnight at 4°C. On the following day, samples were washed and then incubated with PLA probe solution for 1 h at 37°C. Samples were then washed and incubated with the ligation solution for 30 min at 37°C, and then incubated with the amplification solution at 37°C for 100 min. Finally, cells were washed and subjected to another staining cycle with a DAT monoclonal antibody, as previously described. Cell nuclei were counterstained with Hoechst 33258 dye, mounted and analyzed by using a confocal microscope.

Thioflavin-S and α-syn double staining

For staining with thioflavin-S, mouse ventral mesencephalic neurons were incubated with 0.05% of thioflavin-S (Sigma-Aldrich) in PBS, washed three times for 10 min in 80% EtOH and then blocked for subsequent immunostaining with the antibody against α-syn. Cell nuclei were counterstained with Hoechst 33258 dye.

Open-field behavioral tests

Acute locomotor activity of 12-month-old C57BL/6J and C57BL/6JOlaHsd mice after cocaine or GBR-12935 injection (n=8 for each group) was assessed using the automated AnyMaze video tracking system (Stoelting, Wood Dale, IL). The total distance travelled was recorded automatically in the open-field arena (50×50 cm^2), and data were analyzed in 14 trials of 2.5 min each. Mice were gently placed in the arena and were allowed to explore freely for 5 min before starting the test. After 10 min of registration, mice were injected with cocaine (10 mg/kg) (Sigma-Aldrich) or GBR-12935 (10 mg/kg) (Sigma-Aldrich), whereas control mice were treated with vehicle (normal saline 0.9%). All the experiments were conducted during daylight hours.

Vertical microdialysis and high-performance liquid chromatography assays

Extracellular dopamine levels were measured in the striatum using vertical microdialysis coupled to high-performance liquid chromatography assays, according to previously described protocols (Garcia-Reitbock et al., 2010).

Ultrastructural morphological and LR Gold post-embedding immunogold analysis

Glutaraldehyde-fixed cells were evaluated using a standard transmission electron microscopy technique and observed with a transmission electron microscope (FEI Tecnai, Europe NanoPort, Achtseweg Noord 55651 GG Eindhoven, The Netherlands). A comparative study was performed on fixed cells embedded in LR White resin (medium grid). The pellet of cells was cut using an ultramicrotome to obtain ultrathin sections (700 nm) for the post-embedding immunogold analyses. For immunogold staining, ultrathin sections were probed with primary antibodies against synapsin III (rabbit; diluted 1:1000), α-syn (mouse; diluted 1:1000, BD-Bioscience), synapsin Ia/b (mouse; diluted 1:800, Merk-Millipore®) or DAT (rabbit; diluted 1:1000, Santa Cruz Biotechnology) and then with secondary antibodies coupled with gold beads. Sections were contrasted in 1% aqueous uranyl acetate and in 0.3% lead citrate. Finally, sections were observed with a transmission electron microscope (FEI Tecnai). For the analysis of the spatial distribution of synaptic vesicles, the position of each synaptic vesicle was located using ImageJ (National Institutes of Health), and the coordinates were transferred to CrimeS-tat (Ned Levine and Associates) to calculate the number of vesicles per µm. The average size of the immunogold-labeled area, shown as silver-enhanced black grains, was measured within synaptic terminals by using ImageJ. The size of a synapsin-III-positive grain in the C57BL/6J synapses typically ranged from 2 to 10 nm owing to the variable amount of silver build-up around the 1.4-nm gold particle. Owing to inherent variability in cell cultures and different intensities of labeling from different runs of immunocytochemistry processing, all morphometric comparisons between control and depolarized neurons were made between sister cultures, which were processed in parallel as a single experiment. Data points from different experiments were used when the resulting labeling intensities were similar.

Statistical analysis

Differences in the percentage average size of α-syn-, DAT-, synapsin-Ia/b- and synapsin-III-positive areas and between the total levels of control, α-syn-siRNA and SCR-siRNA-treated SH-SY5Y cells and primary mouse mesencephalic neurons in basal and glucose-deprived conditions were assayed by using one-way ANOVA followed by Tukey's multiple comparison test. Likewise, we analyzed the differences in the densities of α-syn and synapsin-Ia/b staining, and their levels in glucose-deprived C57BL/6J cells that had been subjected to transfection with the SCR siRNA or silencing of the synapsin III gene, as well as the total levels of α-syn, DAT, synapsin Ia/b and synapsin III in striatal extracts and upon striatal dopamine release from 12-month-old C57BL/6J and C57BL/6JOlaHsd mice. Differences in the concentration of synaptic vesicles and in the distribution of synapsin III (by using immunogold labeling), as measured by using transmission electron microscopy, were analyzed by one-way ANOVA following Tukey's multiple comparison test. For behavioral studies, the total distance traveled between saline-injected controls and cocaine- or GBR-12935-treated animals for each strain was compared using two-way ANOVA followed by Bonferroni's post-comparison test. All calculations were performed using GraphPad Prism version 5.00 for Windows (GraphPad Prism Software, San Diego, CA). All data were presented as mean+s.d. Statistical significance was established at $P<0.05$.

Acknowledgements

Professor Marc Caron is gratefully acknowledged for kindly providing the DAT–GFP plasmid. We are grateful to Dr Antonio Lavazza for the precious support during transmission electron microscopy analysis. We thank Dr Alessandro Barbon and Dr Daniela Bonini for the precious help with real-time PCR experiments. Tissue samples and associated clinical and neuropathological data were supplied by the Parkinson's UK Brain Bank, funded by Parkinson's UK, a charity registered in England and Wales (258197) and in Scotland (SC037554).

Competing interests

The authors declare no competing or financial interests.

Author contributions

A.B., P.S. and M.Z. designed the study. M.Z., J.G., L.N. and A.B. conducted the experiments. L.D.C. and M.A.C. performed HPLC assays. M.Z., J.G., S.C., G.F. and R.R. performed TEM analysis. M.Z., A.B., J.G. and C.M. analyzed the data. M.Z. and A.B. performed studies on human samples. A.B., M.Z., L.D.C., R.R., M.P., F.B., M.G.S., C.M. and P.S. wrote the paper. This study was managed by A.B., C.M. and P.S.

Funding

This work was supported by the Fondazione Cariplo [grant number 2009-2633]; the Italian Ministry of Education, University and Scientific Research-PRIN 2008; the Regione Lombardia, Italy NEDD Project [grant number CUPH81J09002660007 supporting A.B., M.Z., J.G., L.N., M.P., P.S. and C.M.]; and the European Action [grant number CM1103 to L.D.C. and M.A.C.]. M.Z. was supported by the Regione Lombardia-Dote Ricerca Applicata [grant number POR FSE 2007-13]. A.B. is grateful to 'Ambrosini Arredamenti SNC' for funding support within the project 'Molecular Mechanisms Associated with Neurodegenerative Diseases'.

Supplementary material

Supplementary material available online at
http://jcs.biologists.org/lookup/suppl/doi:10.1242/jcs.157867/-/DC1

Journal of Cell Science

References

Abeliovich, A., Schmitz, Y., Fariñas, I., Choi-Lundberg, D., Ho, W.-H., Castillo, P. E., Shinsky, N., Verdugo, J. M., Armanini, M., Ryan, A. et al. (2000). Mice lacking alpha-synuclein display functional deficits in the nigrostriatal dopamine system. *Neuron* **25**, 239-252.

Anichtchik, O., Calo, L. and Spillantini, M. G. (2013). Synaptic dysfunction in synucleinopathies. *CNS Neurol. Disord. Drug Targets* **12**, 1094-1100.

Bellani, S., Mescola, A., Ronzitti, G., Tsushima, H., Tilve, S., Canale, C., Valtorta, F. and Chieregatti, E. (2014). GRP78 clustering at the cell surface of neurons transduces the action of exogenous alpha-synuclein. *Cell Death Differ.* **21**, 1971-1983.

Bellucci, A., Collo, G., Sarnico, I., Battistin, L., Missale, C. and Spano, P. (2008). Alpha-synuclein aggregation and cell death triggered by energy deprivation and dopamine overload are counteracted by D2/D3 receptor activation. *J. Neurochem.* **106**, 560-577.

Bellucci, A., Navarria, L., Falarti, E., Zaltieri, M., Bono, F., Collo, G., Grazia, M., Missale, C. and Spano, P. (2011a). Redistribution of DAT/alpha-synuclein complexes visualized by "in situ" proximity ligation assay in transgenic mice modelling early Parkinson's disease. *PLoS ONE* **6**, e27959.

Bellucci, A., Navarria, L., Zaltieri, M., Falarti, E., Bodei, S., Sigala, S., Battistin, L., Spillantini, M., Missale, C. and Spano, P. (2011b). Induction of the unfolded protein response by alpha-synuclein in experimental models of Parkinson's disease. *J. Neurochem.* **116**, 588-605.

Bellucci, A., Zaltieri, M., Navarria, L., Grigoletto, J., Missale, C. and Spano, P. (2012). From alpha-synuclein to synaptic dysfunctions: new insights into the pathophysiology of Parkinson's disease. *Brain Res.* **1476**, 183-202.

Bogen, I. L., Boulland, J.-L., Mariussen, E., Wright, M. S., Fonnum, F., Kao, H.-T. and Walaas, S. I. (2006). Absence of synapsin I and II is accompanied by decreases in vesicular transport of specific neurotransmitters. *J. Neurochem.* **96**, 1458-1466.

Boyer, F. and Dreyer, J.-L. (2007). Alpha-synuclein in the nucleus accumbens induces changes in cocaine behaviour in rats. *Eur. J. Neurosci.* **26**, 2764-2776.

Braak, H., Sastre, M. and Del Tredici, K. (2007). Development of alpha-synuclein immunoreactive astrocytes in the forebrain parallels stages of intraneuronal pathology in sporadic Parkinson's disease. *Acta Neuropathol.* **114**, 231-241.

Brenz Verca, M. S., Bahi, A., Boyer, F., Wagner, G. C. and Dreyer, J.-L. (2003). Distribution of alpha- and gamma-synucleins in the adult rat brain and their modification by high-dose cocaine treatment. *Eur. J. Neurosci.* **18**, 1923-1938.

Burre, J., Sharma, M., Tsetsenis, T., Buchman, V., Etherton, M. R. and Sudhof, T. C. (2010). Alpha-synuclein promotes SNARE-complex assembly in vivo and in vitro. *Science* **329**, 1663-1667.

Busch, D. J., Oliphint, P. A., Walsh, R. B., Banks, S. M. L., Woods, W. S., George, J. M. and Morgan, J. R. (2014). Acute increase of alpha-synuclein inhibits synaptic vesicle recycling evoked during intense stimulation. *Mol. Biol. Cell* **25**, 3926-3941.

Cesca, F., Baldelli, P., Valtorta, F. and Benfenati, F. (2010). The synapsins: key actors of synapse function and plasticity. *Prog. Neurobiol.* **91**, 313-348.

Chadchankar, H. and Yavich, L. (2011). Sub-regional differences and mechanisms of the short-term plasticity of dopamine overflow in striatum in mice lacking alpha-synuclein. *Brain Res.* **1423**, 67-76.

Chadchankar, H., Ihalainen, J., Tanila, H. and Yavich, L. (2011). Decreased reuptake of dopamine in the dorsal striatum in the absence of alpha-synuclein. *Brain Res.* **1382**, 37-44.

Chadchankar, H., Ihalainen, J., Tanila, H. and Yavich, L. (2012). Methylphenidate modifies overflow and presynaptic compartmentalization of dopamine via an alpha-synuclein-dependent mechanism. *J. Pharmacol. Exp. Ther.* **341**, 484-492.

Crowther, R. A., Jakes, R., Spillantini, M. G. and Goedert, M. (1998). Synthetic filaments assembled from C-terminally truncated alpha-synuclein. *FEBS Lett.* **436**, 309-312.

Feng, J., Chi, P., Blanpied, T. A., Xu, Y., Magarinos, A. M., Ferreira, A., Takahashi, R. H., Kao, H. T., McEwen, B. S., Ryan, T. A. et al. (2002). Regulation of neurotransmitter release by synapsin III. *J. Neurosci.* **22**, 4372-4380.

Games, D., Seubert, P., Rockenstein, E., Patrick, C., Trejo, M., Ubhi, K., Ettle, B., Ghassemiam, M., Barbour, R., Schenk, D. et al. (2013). Axonopathy in an alpha-synuclein transgenic model of Lewy body disease is associated with extensive accumulation of C-terminal–truncated alpha-synuclein. *Am. J. Pathol.* **182**, 940-953.

Garcia-Reitbock, P., Anichtchik, O., Bellucci, A., Iovino, M., Ballini, C., Fineberg, E., Ghetti, B., Della Corte, L., Spano, P., Tofaris, G. K. et al. (2010). SNARE protein redistribution and synaptic failure in a transgenic mouse model of Parkinson's disease. *Brain* **133**, 2032-2044.

Garcia-Reitboeck, P., Anichtchik, O., Dalley, J. W., Ninkina, N., Tofaris, G. K., Buchman, V. L. and Spillantini, M. G. (2013). Endogenous alpha-synuclein influences the number of dopaminergic neurons in mouse substantia nigra. *Exp. Neurol.* **248**, 541-545.

Gaugler, M. N., Genc, O., Bobela, W., Mohanna, S., Ardah, M. T., El-Agnaf, O. M., Cantoni, M., Bensadoun, J.-C., Schneggenburger, R., Knott, G. W. et al. (2012). Nigrostriatal overabundance of alpha-synuclein leads to decreased vesicle density and deficits in dopamine release that correlate with reduced motor activity. *Acta Neuropathol.* **123**, 653-669.

Kile, B. M., Guillot, T. S., Venton, B. J., Wetsel, W. C., Augustine, G. J. and Wightman, R. M. (2010). Synapsins differentially control dopamine and serotonin release. *J. Neurosci.* **30**, 9762-9770.

Larsen, K. E., Schmitz, Y., Troyer, M. D., Mosharov, E., Dietrich, P., Quazi, A. Z., Savalle, M., Nemani, V., Chaudhry, F. A., Edwards, R. H. et al. (2006). Alpha-synuclein overexpression in PC12 and chromaffin cells impairs catecholamine release by interfering with a late step in exocytosis. *J. Neurosci.* **26**, 11915-11922.

Lundblad, M., Decressac, M., Mattsson, B. and Bjorklund, A. (2012). Impaired neurotransmission caused by overexpression of alpha-synuclein in nigral dopamine neurons. *Proc. Natl. Acad. Sci. USA* **109**, 3213-3219.

Maiya, R., Ponomarev, I., Linse, K. D., Harris, R. A. and Mayfield, R. D. (2007). Defining the dopamine transporter proteome by convergent biochemical and in silico analyses. *Genes Brain Behav.* **6**, 97-106.

Nemani, V. M., Lu, W., Berge, V., Nakamura, K., Onoa, B., Lee, M. K., Chaudhry, F. A., Nicoll, R. A. and Edwards, R. H. (2010). Increased expression of alpha-synuclein reduces neurotransmitter release by inhibiting synaptic vesicle reclustering after endocytosis. *Neuron* **65**, 66-79.

Porton, B., Wetsel, W. C. and Kao, H.-T. (2011). Synapsin III: role in neuronal plasticity and disease. *Semin. Cell Dev. Biol.* **22**, 416-424.

Prasad, K., Beach, T. G., Hedreen, J. and Richfield, E. K. (2012). Critical role of truncated alpha-synuclein and aggregates in Parkinson's disease and incidental Lewy body disease. *Brain Pathol.* **22**, 811-825.

Qin, Y., Ouyang, Q., Pablo, J. and Mash, D. C. (2005). Cocaine abuse elevates alpha-synuclein and dopamine transporter levels in the human striatum. *Neuroreport* **16**, 1489-1493.

Specht, C. G. and Schoepfer, R. (2001). Deletion of the alpha-synuclein locus in a subpopulation of C57BL/6J inbred mice. *BMC. Neurosci.* **2**, 11.

Spinelli, K. J., Taylor, J. K., Osterberg, V. R., Churchill, M. J., Pollock, E., Moore, C., Meshul, C. K. and Unni, V. K. (2014). Presynaptic alpha-synuclein aggregation in a mouse model of Parkinson's disease. *J. Neurosci.* **34**, 2037-2050.

Tao-Cheng, J.-H. (2006). Activity-related redistribution of presynaptic proteins at the active zone. *Neuroscience* **141**, 1217-1224.

Tofaris, G. K., Reitböck, P. G., Humby, T., Lambourne, S. L., O'Connell, M., Ghetti, B., Gossage, H., Emson, P. C., Wilkinson, L. S., Goedert, M. et al. (2006). Pathological changes in dopaminergic nerve cells of the substantia nigra and olfactory bulb in mice transgenic for truncated human alpha-synuclein(1-120): implications for Lewy body disorders. *J. Neurosci.* **26**, 3942-3950.

Venton, B. J., Seipel, A. T., Phillips, P. E., Wetsel, W. C., Gitler, D., Greengard, P., Augustine, G. J. and Wightman, R. M. (2006). Cocaine increases dopamine release by mobilization of a synapsin-dependent reserve pool. *J. Neurosci.* **26**, 3206-3209.

Volz, T. J., Farnsworth, S. J., Hanson, G. R. and Fleckenstein, A. E. (2008). Methylphenidate-induced alterations in synaptic vesicle trafficking and activity. *Ann. N. Y. Acad. Sci.* **1139**, 285-290.

Yavich, L., Tanila, H., Vepsäläinen, S. and Jäkälä, P. (2004). Role of alpha-synuclein in presynaptic dopamine recruitment. *J. Neurosci.* **24**, 11165-11170.

Supplementary material

Supplementary material figure S1. Immunofluorescent and phase contrast characterization of C57BL/6J and C57BL/6JOlaHsd primary mesencephalic neuronal cell cultures at 10 DIV; Thioflavin-S/alpha-syn double staining and quantification of DAT immunopositive area; **Double immunofluorescence labelling in the human caudate putamen.**

A. β3-Tubulin immunolabeling; **B**. MAP2 immunolabeling; **C**. Synaptophysin immunolableing; **D**. Phase contrast images. **E**. Thioflavin S/α-syn double labelling in control and GD-exposed primary mesencephalic neurons from C57BL/6J mice. Please note the presence of thioflavin-S + α-syn-positive inclusions in the cell bodies and processes of GD exposed cells that is indicative of α-syn fibrillary aggregation. **F**. Quantification of the % average size of DAT immunopositive area in primary mouse mesencephalic dopaminergic neurons from C57BL/6J and C57BL/6JOlaHsd mice. * $P < 0.05$, One-way ANOVA + Tukey's Multiple comparison test. **G**. Quantification of the % average size of DAT immunopositive area in primary mouse mesencephalic dopaminergic neurons from control or α-syn siRNA-exposed primary mouse mesencephalic dopaminergic neurons from C57BL/6J mice. * $P < 0.05$, One-way ANOVA + Tukey's Multiple comparison test. **H.** Double immunofluorescent labelling for synapsin III and α-syn in the caudate putamen of a PD patient and age matched control. **I**. Double immunofluorescent labelling for synapsin III and synaptophysin in the caudate putamen of a PD patient and age-matched control. Scale bars: A: 60 μm for A-C; D: 200 μm. Big scale bar in E: 100 μm; small scale bar in E: 10 μm. H: 200 μm for H,I.

Supplementary material figure S2. Triple immunofluorescent labelling and synapsin Ia/b immunopositive area quantification

A. Triple immunofluorescent labelling of DAT, α-syn and synapsin III or synapsin Ia/b in primary C57BL/6J, C57BL/6JOlaHsd as well as SCR or α-syn siRNA-exposed mesencephalic neurons under basal conditions or after GD. Big scale bar: 100 μm; small scale bar: 5 μm. **B**. Quantification of the % average size of synapsin Ia/b immunopositive area in primary mouse mesencephalic dopaminergic neurons from C57BL/6J and C57BL/6JOlaHsd mice. **C**. Quantification of the % average size of synapsin Ia/b immunopositive area in SCR or α-syn siRNA-exposed primary mouse mesencephalic dopaminergic neurons from C57BL/6J mice.

Supplementary material figure S3. Immunoblotting in SH-SY5Y cell extracts and triple immunofluorescent stainings in DAT-GFP SH-N-SK cells and primary mesencephalic neurons

A. Representative immunoblotting from SCR and α-syn siRNA-exposed dopaminergic differentiated SH-SY5Y cells under basal conditions and after GD exposure. GAPDH immunopositive bands are reported as a control for equal loading. **B-E**. Levels of α-syn (**B**), DAT (**C**), synapsin Ia/b (**D**) and synapsin III (**E**) in SCR and α-syn siRNA-exposed SH-SY5Y cells under basal conditions and after GD. * P<0.05 One-way ANOVA + Tukey's Multiple comparison test. **F-G**. Double immunofluorescent labelling of synapsin III/α-syn and synapsin Ia/b/α-syn in DAT-GFP-SK-N-SH stable cell clones transfected with human SYN120 α-syn. Please note the presence of synapsin III/DAT/α-syn- (arrow) and synapsin Ia/b/DAT/α-syn-positive (arrowhead) inclusions in these cells while in mock cells the proteins were mainly localized to the plasma membrane. Scale bar: 40 µm. **H**. Triple immunofluorescent labelling of synapsin Ia/b, DAT and α-syn in primary control, GD-treated, GD + SCR or GD + synapsin III siRNA-exposed C57BL/6J mesencephalic neurons. Scale bar: 100 µm. **I**. Graph showing the changes in % ΔCt values indicative of the relative expression of α-syn mRNA in C57BL/6J, C57BL/6J + scramble, C57BL/6J + α-syn siRNA and GD-exposed C57BL/6J primary mesencephalic neurons. * + 56 % $P < 0.001$ vs C57BL/6J + SCR and ° -35.63 % $P < 0.001$ vs C57BL/6J, One-way ANOVA + Tukey's Multiple comparison test. **J**. Graph showing the changes in % ΔCt values indicative of relative expression of synapsin III mRNA in C57BL/6J, C57BL/6JOlaHsd, C57BL/6J + scr, C57BL/6J + synapsin III siRNA and GD-exposed C57BL/6J primary mesencephalic neurons. * - 61.99 % $P < 0.001$ vs C57BL/6J, ° - 60.42 % $P < 0.001$ vs C57BL/6J, * - 58.87 % $P < 0.001$ vs C57BL/6J, One-way ANOVA + Tukey's Multiple comparison test.

Supplementary material figure S4. TEM Immunogold labelling

Transmitted electron microscopy immunogold labelling of α-syn (**A**), synapsin Ia/b (**B**) and DAT (**C**) in primary mouse mesencephalic neurons from C57BL/6J and C57BL/6JOlaHsd mice. Arrows indicate the area of immunogold-positive labelling. Figure glossary: Mee: pre-synaptic membrane; Mps: post-synaptic membrane. **D**. Representative image showing the immunolabelling with human recombinant synapsin III-pre-adsorbed anti-synapsin III antibody in the caudate/putamen of one of the PD brain analysed for this study. **E**. Representative image showing synapsin Ia/b immunolabeling in the caudate/putamen of a PD patient and age matched control. Scale bars: A: 25 nm; B: 200 nm; C: 150 nm. D: 200 µm for D,E.

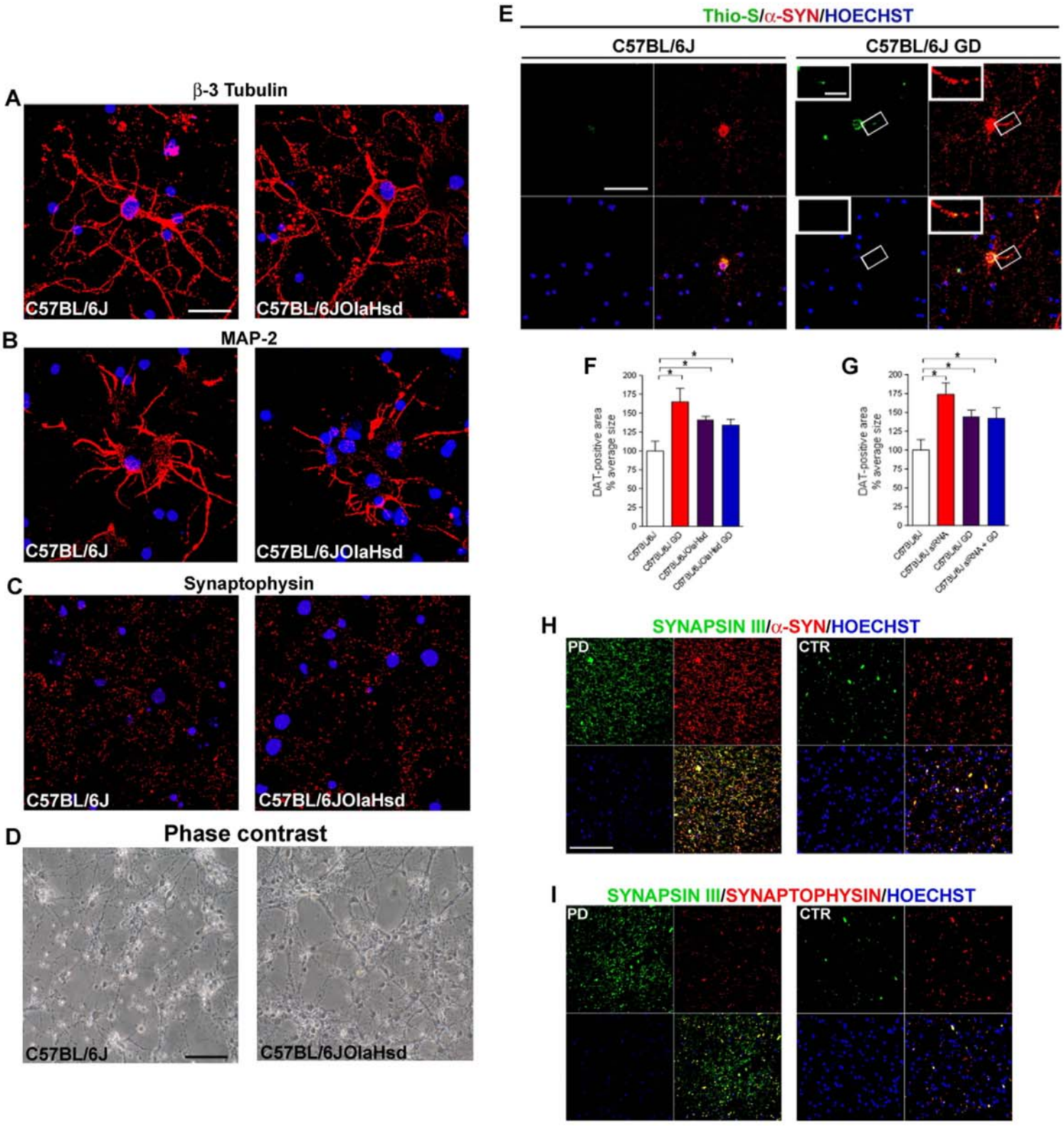

Supplementary material Fig. S1

Supplementary material Fig. S2

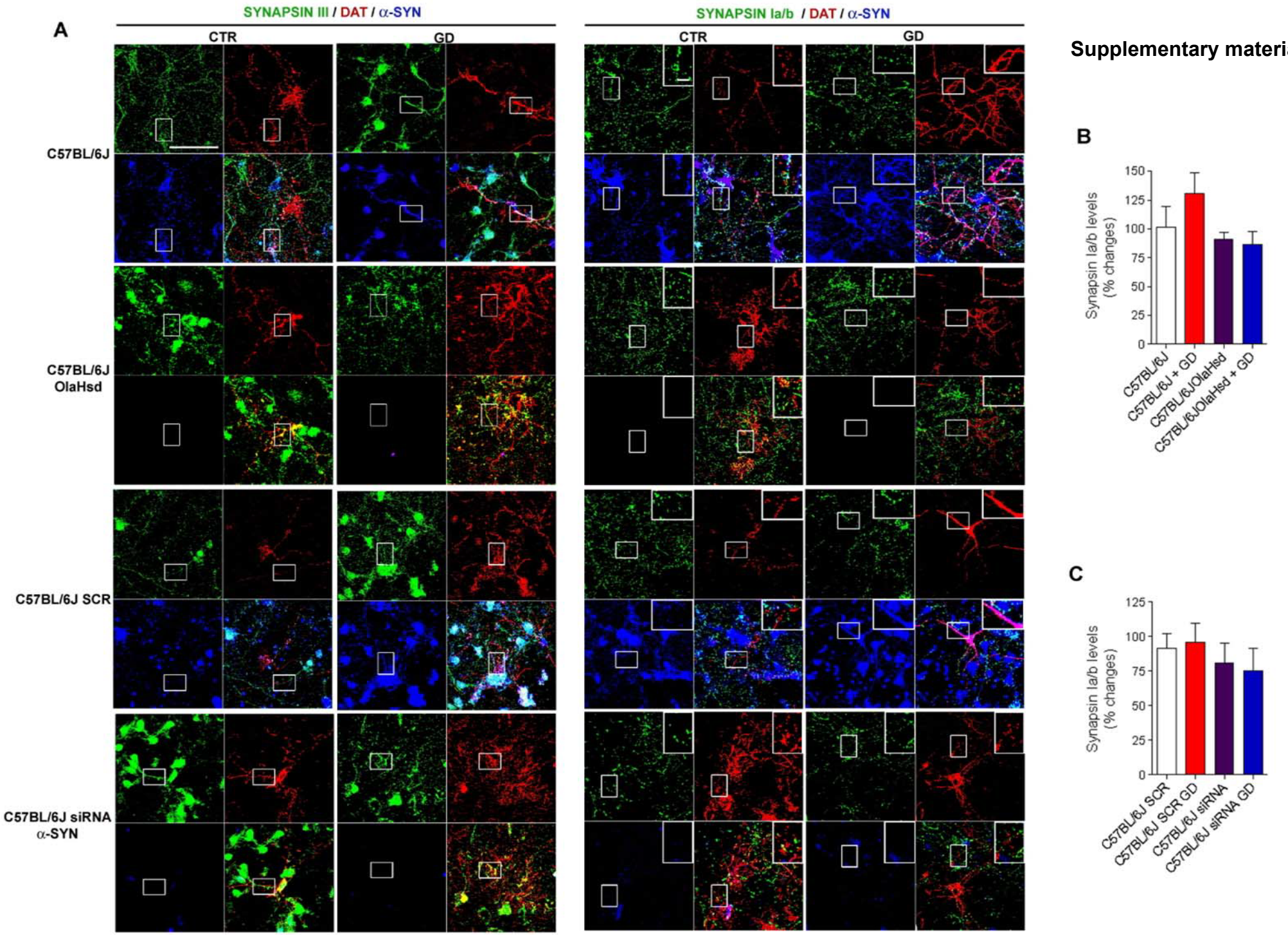

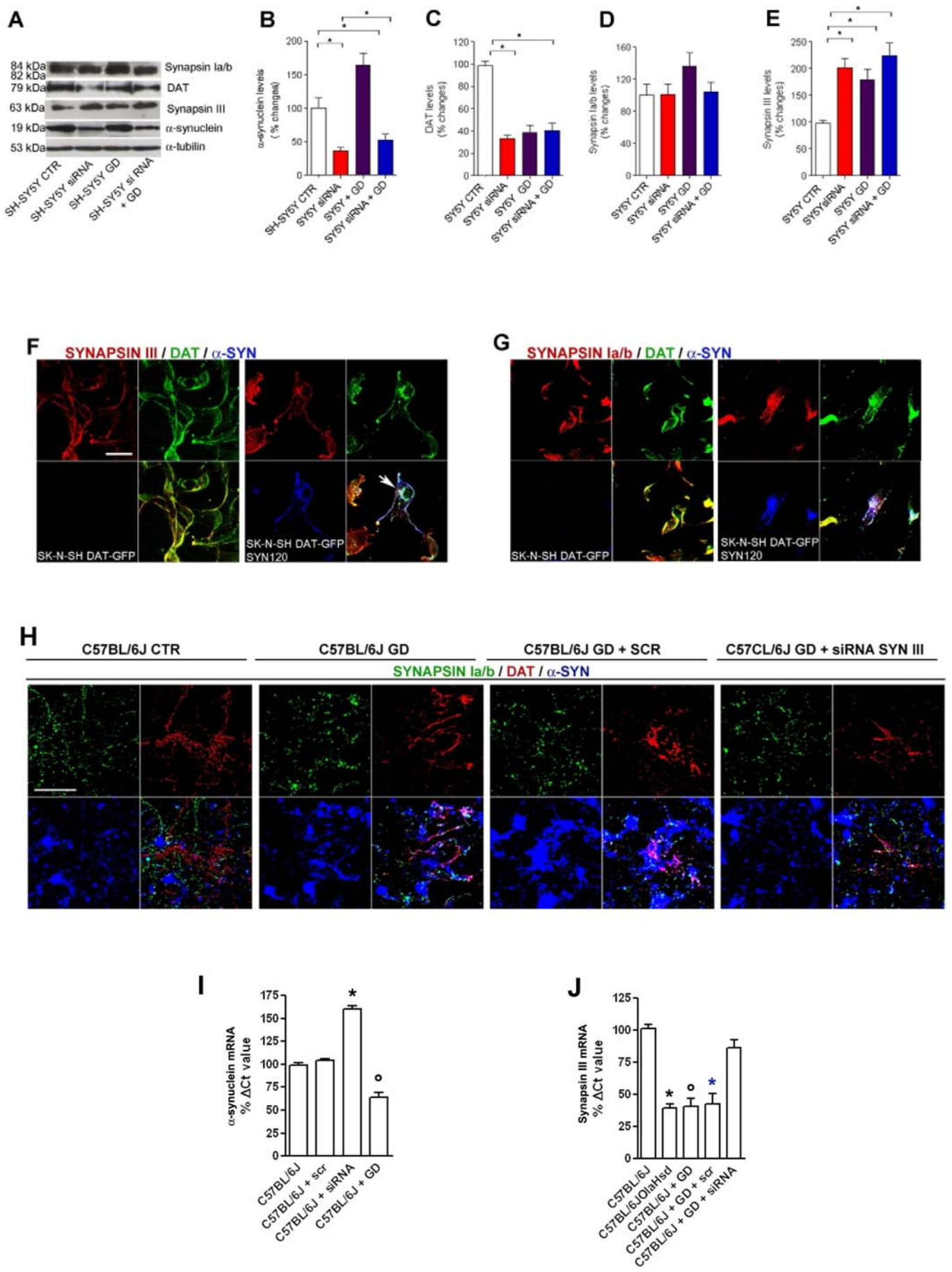

Supplementary material Fig. S3

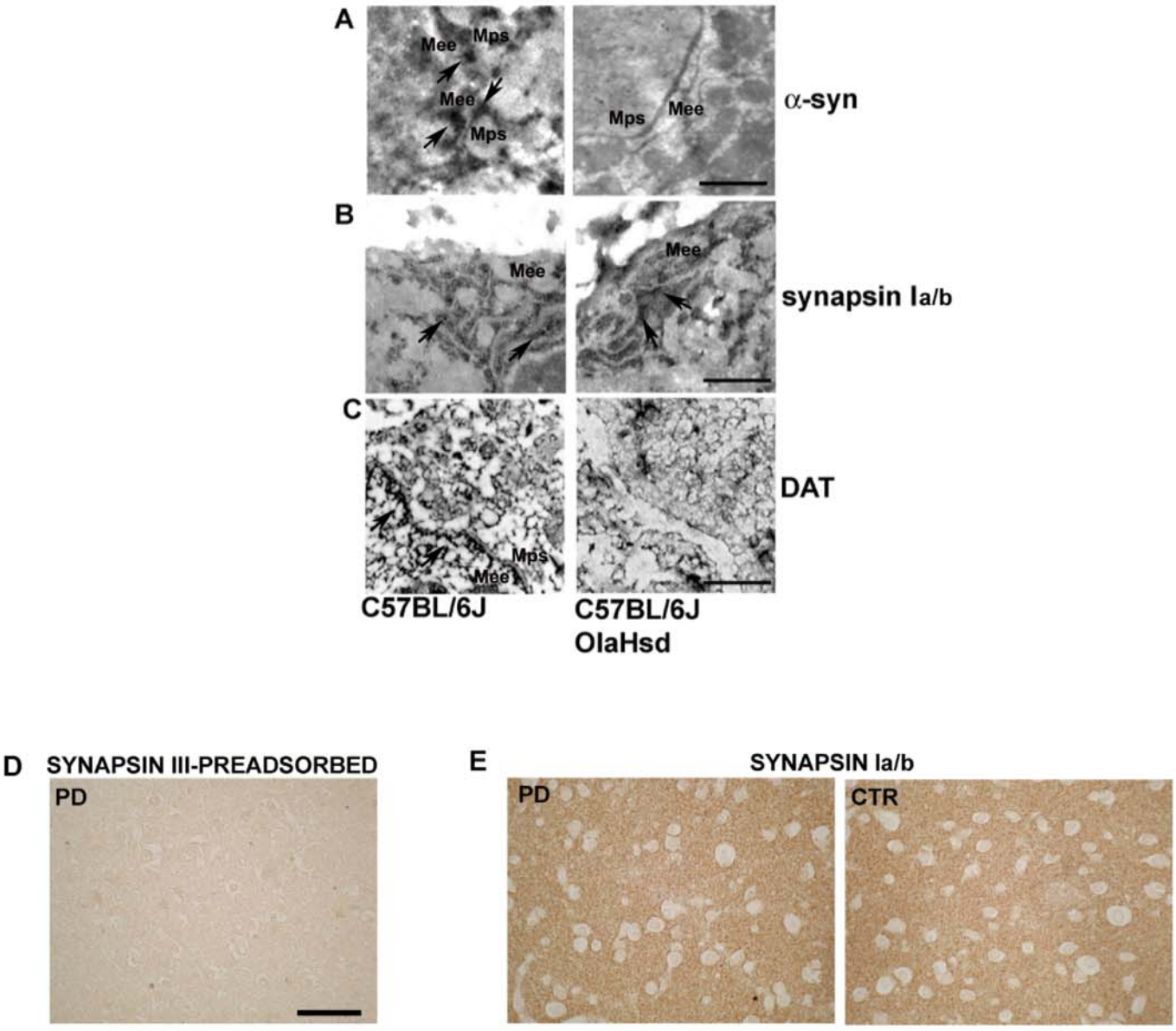

Supplementary material Fig. S4